ICES REPORT 14-09

May 2014

Isogeometric contact: a review

by

L. De Lorenzis, P. Wriggers, T.J.R. Hughes

The Institute for Computational Engineering and Sciences
The University of Texas at Austin
Austin, Texas 78712

Reference: L. De Lorenzis, P. Wriggers, T.J.R. Hughes, "Isogeometric contact: a review," ICES REPORT 14-09, The Institute for Computational Engineering and Sciences, The University of Texas at Austin, May 2014.

Isogeometric contact: a review

L. De Lorenzis, P. Wriggers, T.J.R. Hughes

Abstract

This paper reviews the currently available computational contact formulations within the framework of isogeometric analysis (IGA). As opposed to conventional Lagrange discretizations, IGA basis functions feature higher and tailorable inter-element continuity, which translates into evident advantages for the description of interacting surfaces, especially in presence of large displacements and large sliding. This has recently motivated the proposal of several isogeometric contact treatments, based on different ways to incorporate the contact contribution into the variational form of a continuum mechanics problem and to formulate its discretized version. After a brief overview of conventional and isogeometric basis functions as well as conventional contact mechanics approaches, the available isogeometric contact formulations are examined. Attention is paid to the favorable and unfavorable features they share with their finite element counterparts, as well as to the consequences stemming from the use of IGA basis functions. The main needs for future research emerging from the current state of the art are outlined.

Keywords: contact mechanics, interface modeling, isogeometric analysis, NURBS, smoothing, state of the art review.

1 Introduction

Isogeometric analysis (IGA) was recently introduced by Hughes and coworkers (Hughes et al., 2005, Cottrell et al. 2009) with the primary original purpose to enable a tighter connection be-

tween computer aided geometric design (CAGD) and finite element analysis (FEA). By simplifying the cost-intensive computational model generation process, involving geometry clean-up, feature removal and mesh generation required for standard FEA, and leading to a seamless integration of CAGD and FEA tools, IGA meant to reduce or eliminate the major bottleneck in engineering analysis procedures. Within the IGA framework, the same smooth and higher order basis functions, e.g., non-uniform rational B-splines (NURBS) or T-splines, are used for the representation of the exact CAD geometry and for the approximation of the FEA solution fields.

Independently from the achievement of the original goal, IGA turned out to exhibit increased accuracy and robustness on a per-degree-of-freedom basis in comparison to standard finite element methods (FEM) (Evans et al. 2009, Großmann et al. 2012) and to deliver a number of additional advantages in several areas of computational mechanics. Contact mechanics, which is the focus of the present paper, is one of these areas. Here the higher order and higher and tailorable continuity of IGA basis functions lead to evident potential advantages in the description of interacting surfaces undergoing large displacements and large sliding, as recognized already in the first IGA paper (Hughes et al. 2005). Thus, several computational contact formulations within the IGA framework have been developed in the past few years. Clearly, the majority of these formulations directly originate from the contact treatments currently available in the realm of FEM. As a result, they share the favorable and unfavorable sides of their FEM counterparts, while taking advantage of the specific properties of IGA basis functions.

The purpose of this paper is to summarize the main documented contributions in the field of isogeometric contact and thus derive a systematic classification of the tested isogeometric formulations, along with their FEM counterparts. Such a classification goes hand in hand with the exploration of the desirable and undesirable features of the various formulations, which in turn naturally leads to the definition of future research needs in the framework of isogeometric contact. Throughout the paper, the focus is on large deformation contact in quasi-static conditions using implicit methods, unless otherwise specified. The paper is organized as follows: Section 2 comparatively reviews the main properties of the basis functions used in IGA and FEM, with special emphasis on the prop-

erties relevant for contact computations. Section 3 reviews the main contact treatments within the FEM framework, devoting special attention to the FEM counterparts of available IGA contact formulations. The main drawbacks stemming from non-smooth discretizations are highlighted and the remedies proposed before the advent of IGA are briefly reviewed. Section 4 presents the currently available isogeometric contact formulations and points out their similarities and differences with respect to their FEM counterparts. The well-known Hertz example is revisited to exemplify the influence of each single property of IGA basis functions on results. A rotating ironing example is also briefly illustrated. In Section 5, isogeometric domain decomposition approaches as well as extensions and applications of isogeometric contact formulations are reviewed. Finally, suggestions for research needs emerging from the previous review are set forth in Section 6 which concludes the paper.

2 Basis functions and parameterizations in FEM and IGA: main properties and differences

In this section we overview the main properties of the most common basis functions used in FEM and IGA and of the corresponding parameterizations applied for the discretization of the continuum geometry. In both FEM and IGA, uni- and bi-variate parameterizations represent contact curves/surfaces respectively in 2D and 3D settings, and these are inherited respectively from the bi- and tri-variate parameterizations of the continuum in a straightforward fashion. In the following, d_s and d_p denote the dimensions of the physical and of the parametric space, respectively. Within an isoparametric approach, the same parameterizations are adopted for the field of the unknowns. In the large deformation framework, this leads to a significant impact of the properties of the basis on the quality of the results.

For FEM, classical and hierarchical Lagrange basis functions are touched upon. Further details can be found e.g. in Szabó and Babuška 1991, Szabó et al. 2004. The IGA overview includes Bernstein, B-spline and NURBS basis functions with the corresponding Bézier, B-spline and NURBS

parameterizations. Although IGA is based on NURBS, examination of their antecedents serves to elucidate the role of single properties of the basis functions on the results of contact analyses (see Section 4.5). Further details and extensive references can be found in Piegl and Tiller (1996) and Rogers (2001). For the sake of completeness, isogeometric parameterizations enabling local refinement are mentioned along with relevant references.

2.1 Lagrange, Bernstein/Bézier, B-spline and NURBS basis functions and parameterizations

2.1.1 Lagrange basis functions and parameterizations

The classical univariate Lagrange basis functions on the parametric domain $-1 \leq \xi \leq 1$ are given by

$$L_{i,p}(\xi) = \prod_{j=1, j\neq i}^{p+1} \frac{\xi - \xi_j}{\xi_i - \xi_j} \tag{1}$$

with $i = \{1, 2, ..., p+1\}$ and p as the polynomial degree. The points ξ_j where

$$L_{i,p}(\xi_j) = \delta_{ij} \tag{2}$$

with δ_{ij} as the Kronecker's delta, are called *nodes*. These are polynomial functions which constitute a partition of unity, i.e. $\sum_{i=1}^{p+1} L_{i,p}(\xi) = 1$ for all $-1 \leq \xi \leq 1$. They assume both positive and negative values within the domain. Due to eq. (2), the basis is interpolatory at the nodes.

Every function that can be represented as a linear combination of the standard Lagrange basis can also be represented by a set of hierarchical basis functions, whereby all lower-order functions are contained in the higher order basis (Szabó and Babuška 1991). Hierarchic approximation spaces are created by using the tensor product space of integrated Legendre polynomials. Thus, different polynomial degrees can be used in each spatial direction to obtain anisotropic approxima-

tion spaces. Compared to Lagrange polynomials, these hierarchic shape functions lead to better conditioned system matrices.

Contrary to the classical h-version of the FEM, the p-version (Szabó and Babuška 1991, Szabó et al. 2004) reduces the error of the approximation by increasing the polynomial degree of the shape functions locally or globally, and not by refining the mesh. Enlarging the element dimensions requires special attention to the representation of curved boundaries. These can be described exactly using the blending function method (Gordon and Hall 1973, Szabó and Babuška 1991, Düster et al. 2001), which introduces a non-isoparametric mapping.

Both classical and hierarchical Lagrange parameterizations achieve C^0 continuity at the inter-element boundary, which in an isoparametric context applies to both the geometry and the unknown displacement field. With the blending function method, geometric continuity at the boundary of the domain depends on that of the exact geometry, whereas the displacement approximation is still C^0 continuous.

2.1.2 Bernstein basis functions and Bézier parameterizations

A Bernstein polynomial basis of degree p is defined as

$$B_{i,p}(\xi) = \frac{p!}{(i-1)!\,(p-i+1)!}\xi^{i-1}(1-\xi)^{p-i+1} \tag{3}$$

with $i = \{1, 2, ..., p+1\}$, on the parametric domain $0 \leq \xi \leq 1$. These are polynomial functions which constitute a partition of unity, i.e. $\sum_{i=1}^{p+1} B_{i,p}(\xi) = 1$ for all $0 \leq \xi \leq 1$. They are point-wise non-negative, i.e. $B_{i,p}(\xi) \geq 0$ for all i, p and $0 \leq \xi \leq 1$. It is $B_{1,p}(0) = B_{p+1,p}(1) = 1$, i.e., the basis is interpolatory at the ends of the domain.

Multivariate Bernstein basis functions are generated through the tensor product of the univariate ones. Denoting the univariate basis functions in each parametric direction $d = 1...d_p$ as $B^d_{i_d,p_d}$, the multivariate basis functions $B_{\mathbf{i},\mathbf{p}}(\boldsymbol{\xi})$ are obtained from

$$B_{\mathbf{i},\mathbf{p}}(\xi) = \prod_{d=1}^{d_p} B^d_{i_d,p_d}\left(\xi^d\right) \tag{4}$$

where the multi-index $\mathbf{i} = \left\{i_1, ..., i_{d_p}\right\}$ denotes the position in the tensor product structure, $\mathbf{p} = \{p_1, ..., p_d\}$ indicates the polynomial degree, and $\boldsymbol{\xi} = \left\{\xi^1, ..., \xi^{d_p}\right\}$ is the vector of the parametric coordinates in each parametric direction d. Tensor product multivariate basis functions inherit all the key features of their univariate progenitors. Once the Bernstein basis functions are available, a Bézier curve can be constructed as their linear combination

$$\mathbf{C}(\xi) = \sum_{i=1}^{p+1} \mathbf{P}_i B_{i,p} \tag{5}$$

where $\mathbf{P}_i \in \mathbb{R}^{d_s}$ are the so-called control points. Bézier surfaces and solids are obtained for $d_p = 2$ and $d_p = 3$, respectively, from a linear combination of multivariate Bernstein basis functions and control points as follows

$$\mathbf{S}(\boldsymbol{\xi}) = \sum_{\mathbf{i}} \mathbf{P}_{\mathbf{i}} B_{\mathbf{i},\mathbf{p}}(\boldsymbol{\xi}) \tag{6}$$

where the summation is extended to all combinations of the multi-index $\mathbf{i}$. Bézier curves (surfaces, solids) are a special case of B-spline curves (surfaces, solids) described in the next sub-section.

The combination of some of the basis function properties leads to interesting additional properties, namely:

- the convex hull property. A Bézier curve is completely contained within the convex hull defined by its control points. For a curve of degree p, the convex hull is defined as the union of all of the convex hulls formed by $p + 1$ successive control points. The same property is also possessed by Bézier surfaces;
- the variation diminishing property. No plane has more intersections with a Bézier curve than it has with its control polygon. Interestingly, there is no known variation diminishing

property for surfaces.

2.1.3 B-spline basis functions and parameterizations

A B-spline basis of degree p is generated based on a sequence of real numbers called a knot vector

$$\Xi = \{\xi_1, ..., \xi_{m+p+1}\} \tag{7}$$

where $\xi_1 \leq \xi_2 \leq ... \leq \xi_{m+p+1}$, each $\xi_j \in \mathbb{R}$ is a knot, and m is the number of basis functions. Moreover $m - p$ is the number of inner knot spans, some of which may possibly have zero length if they are bounded by repeated inner knot vector entries. In the so-called open knot vectors, the first $p + 1$ knots are equal and the last $p + 1$ terms are equal. Very often $\xi_1 = 0$ and $\xi_{m+p+1} = 1$.

Based on the knot vector Ξ and order p, the univariate B-spline basis functions $\mathcal{B}_{i,p}(\xi)$ with $i = \{1, 2, ..., m\}$ are obtained from the so-called Cox-de Boor recursion formula (Piegl and Tiller 1996). Starting from $p = 0$ where

$$\mathcal{B}_{i,0}(\xi) = \begin{cases} 1 & \xi_i \leq \xi < \xi_{i+1} \\ 0 & \text{otherwise} \end{cases} \tag{8}$$

the basis functions for $p > 0$ are obtained from

$$\mathcal{B}_{i,p}(\xi) = \frac{\xi - \xi_i}{\xi_{i+p} - \xi_i}\mathcal{B}_{i,p-1}(\xi) + \frac{\xi_{i+p+1} - \xi}{\xi_{i+p+1} - \xi_{i+1}}\mathcal{B}_{i+1,p-1}(\xi) \tag{9}$$

introducing the convention $0/0 = 0$. These functions are piecewise polynomials and some of their important properties are summarized below. They constitute a partition of unity, i.e. $\sum_{i=1}^{m} \mathcal{B}_{i,p}(\xi) = 1$ for all $\xi_1 \leq \xi \leq \xi_{m+p+1}$. They are point-wise non-negative over the entire domain, i.e. $\mathcal{B}_{i,p}(\xi) \geq 0$ for all i, p, and $\xi_1 \leq \xi \leq \xi_{m+p+1}$. Their continuity depends on Ξ only. If Ξ has no repeated interior knot, then the order-p basis functions $\mathcal{B}_i$ have continuity C^{p-1} at the knots. If a knot has multiplicity k, the smoothness of the B-spline basis is C^{p-k} at that knot.

When the multiplicity of a knot is exactly p, the continuity of the basis function becomes C^0 and the basis becomes interpolatory at that knot. In particular, open knot vectors lead to a basis that is interpolatory at the ends of the domain. Finally, they have local support, meaning that the support of an order-p basis function is always $p+1$ knot spans.

Multivariate B-splines are generated through the tensor product of univariate B-splines. In a d_p-dimensional parametric space, d_p univariate knot vectors are needed

$$\Xi^d = \left\{\xi_1^d, ..., \xi_{m_d+p_d+1}^d\right\} \tag{10}$$

where p_d is the polynomial degree in the parametric direction d, and m_d is the associated number of basis functions. Denoting the univariate basis functions in each parametric direction d as $\mathcal{B}_{i_d,p_d}^d$, the multivariate basis functions $\mathcal{B}_{\mathbf{i},\mathbf{p}}(\boldsymbol{\xi})$ are obtained from

$$\mathcal{B}_{\mathbf{i},\mathbf{p}}(\xi) = \prod_{d=1}^{d_p} \mathcal{B}_{i_d,p_d}^d\left(\xi^d\right) \tag{11}$$

Once again tensor product multivariate basis functions inherit all the key features of their univariate progenitors.

Note that, within IGA, in the univariate case one knot span plays the role of an element in standard FEM. Therefore, unlike Lagrange and Bézier basis functions which have support on one element, the B-spline basis is defined globally on a patch (i.e. the collection of a number of elements $m-p$ equal to the number of knot spans in the knot vector) and each function has support on $p+1$ elements. Elements may have zero size if they are bounded by repeated knots. In the multivariate case, the quantity $\prod_{d=1}^{d_p}(m_d - p_d)$ is the number of elements defined by the parameterization, some of which may possibly have zero area if they are bounded by repeated inner knot vector entries in at least one parametric direction. These elements are referred to as Bézier elements. Each basis function has support on $\prod_{d=1}^{d_p}(p_d+1)$ elements.

Once the B-spline basis functions are available, a B-spline curve can be constructed as their linear

combination

$$\mathbf{C}(\xi) = \sum_{i=1}^{m} \mathbf{P}_i \mathcal{B}_{i,p} \tag{12}$$

B-spline surfaces and solids are obtained for $d_p = 2$ and $d_p = 3$, respectively, from a linear combination of multivariate B-spline basis functions and control points

$$\mathbf{S}(\boldsymbol{\xi}) = \sum_{\mathbf{i}} \mathbf{P}_{\mathbf{i}} \mathcal{B}_{\mathbf{i},\mathbf{p}}(\boldsymbol{\xi}) \tag{13}$$

where the summation is extended to all combinations of the multi-index $\mathbf{i}$. From the properties of the B-spline basis functions follow analogous properties of B-spline curves and surfaces. In general, in all these entities there will be at least as many continuous partial derivatives in parametric direction d across an element boundary as the basis functions have across the corresponding knot value in Ξ^d. Another property inherited from the basis is that of locality: due to the compact support of the basis functions, moving a single control point will affect the geometry of no more than $\prod_{d=1}^{d_p}(p_d + 1)$ elements. Also, B-spline curves and surfaces possess the convex hull property such as Bézier curves and surfaces, and B-spline curves possess the variation diminishing property such as Bézier curves.

2.1.4 NURBS basis functions and parameterizations

The main reason why NURBS are introduced is that, unlike B-splines, they allow for an exact construction of conic sections such as circles and ellipses. NURBS basis functions are obtained from a projective transformation of their B-spline progenitors in $\mathbb{R}^{d_s+1}$. Univariate NURBS basis functions $N_{i,p}(\xi)$ are given by

$$N_{i,p}(\xi) = \frac{w_i \mathcal{B}_{i,p}(\xi)}{\sum_{j=1}^{m} w_j \mathcal{B}_{j,p}(\xi)} \tag{14}$$

where $\mathcal{B}_{i,p}$ are B-spline basis functions and $w_i > 0$ are the corresponding weights. NURBS basis functions inherit the key features of their B-splines progenitors, namely, partition of unity, pointwise non-negativity, and local support over $p+1$ knot spans. Also, their continuity in each parametric direction follows from the knot vectors Ξ^i exactly as illustrated for univariate B-spline basis functions. Multivariate NURBS basis functions are also obtained in tensor product form as

$$N_{\mathbf{i},\mathbf{p}}\left(\boldsymbol{\xi}\right) = \frac{w_{\mathbf{i}}\mathcal{B}_{\mathbf{i},\mathbf{p}}\left(\boldsymbol{\xi}\right)}{\sum_{\mathbf{j}} w_{\mathbf{j}}\mathcal{B}_{\mathbf{j},\mathbf{p}}\left(\boldsymbol{\xi}\right)} \tag{15}$$

Also in this case, tensor product multivariate basis functions inherit all the key features of their univariate progenitors. The parameterization defines $\prod_{d=1}^{d_p}\left(m_d - p_d\right)$ Bézier elements, with each basis function having support on $\prod_{d=1}^{d_p}\left(p_d+1\right)$ elements.

Once the NURBS basis functions are available, a NURBS curve can be constructed as their linear combination

$$\mathbf{C}\left(\xi\right) = \sum_{i=1}^{m} \mathbf{P}_i N_{i,p} \tag{16}$$

NURBS surfaces and solids are obtained for $d_p = 2$ and $d_p = 3$, respectively, as follows

$$\mathbf{S}\left(\boldsymbol{\xi}\right) = \sum_{\mathbf{i}} \mathbf{P}_{\mathbf{i}} N_{\mathbf{i},\mathbf{p}}\left(\boldsymbol{\xi}\right) \tag{17}$$

Finally, NURBS curves and surfaces possess the same continuity, locality, and convex hull properties illustrated earlier for Bézier and B-spline curves and surfaces. Also, NURBS curves possess the variation diminishing property such as Bézier and B-spline curves.

2.1.5 Summary

Table 1 summarizes the main properties of the basis functions overviewed in this section, whereas Figure 1 illustrates an example of basis functions with $p = 2$ corresponding to a parametric domain $[0, 1]$ subdivided into two equal elements. Using the Lagrange and Bernstein bases, $p+1$

functions are defined on each element, whereas in the B-spline and NURBS parameterizations the two elements constitute a patch defined by the knot vector $\Xi = \{0\,0\,0\,0.5\,1\,1\,1\}$, on which $m = 4$ basis functions are defined. The properties of the basis functions indicated in Table 1 are clearly observable in the figure, and the comparison between Figures 1b and 1c demonstrates the role of the weights chosen for the NURBS basis functions.

2.2 Isogeometric parameterizations with local refinement capabilities

Due to their tensor product nature, NURBS parameterizations are not amenable to local refinement. In order to overcome this limitation, several alternative technologies have been proposed. While a detailed examination of the available options is outside the scope of this contribution, the most developed techniques at the current state of research are analysis-suitable T-splines (Bazilevs et al 2010, Scott et al. 2012), hierarchical B-splines (Vuong et al. 2011, Schillinger et al. 2012) and the recently proposed isogeometric spline forests (Scott et al. 2014). T-splines have already been tested for contact computations, as will be illustrated later.

Implementationally convenient NURBS and T-spline finite element data structures are derived from the Bézier extraction concept (Borden et al. 2011, Scott et al. 2011). As in traditional finite element analysis, the extracted Bézier elements are defined in terms of a fixed set of polynomial basis functions, the so-called Bernstein basis. The Bézier elements may be processed in the same way as in a standard finite element computer program, utilizing exactly the same data processing arrays. In fact, only the shape function subroutine needs to be modified, all other aspects of a finite element program remaining the same. A byproduct of the extraction process is the element extraction operator. This operator localizes the topological and global smoothness information to the element level, and represents a canonical treatment of T-junctions, referred to as "hanging nodes" in finite element analysis and a fundamental feature of T-splines.

3 Before IGA: contact formulations for C^0 discretizations and smoothing techniques

Despite the progress made in the implementation of contact algorithms in commercial codes, the efficient numerical solution of large deformation, large slip multi-body contact problems is still a significant challenge and thus intense research is still going on in the area of computational contact mechanics (Wriggers and Zavarise 2011). The main difficulties are related to high non-linearity and non-smoothness, potential ill-conditioning, and heavy computational costs associated with contact detection.

Treatment of contact constraints within either FEM or IGA entails two main aspects. The first aspect is the choice of the method to be used for the enforcement of the contact constraints, the most popular options being the Lagrange multiplier method, the penalty method and combinations of these two such as augmented Lagrange methods. Well-known drawbacks of penalty-based formulations are unphysical penetrations and bad conditioning of the system of equations. On the other hand, the Lagrange multiplier method and the augmented Lagrange multiplier approach in the form proposed by Alart and Curnier (1991) introduce additional unknowns, whereas the augmented Lagrange multiplier method based on Uzawa's algorithm requires an additional augmentation loop. Many more details can be found in the classical textbooks by Laursen (2002) and Wriggers (2006). Any of the aforementioned methods can be used in combination with any of the formulations presented in the next sections, regardless of whether FEM or IGA discretizations are used. Therefore this aspect will not be further explored in this paper.

The second aspect is the choice of the way the contact surfaces are parameterized, incorporated into the variational formulation of the problem and discretized. The importance of this topic is driven by the need to cope with non-conforming discretizations across contacting boundaries and/or large deformation and large sliding cases. This paper focuses on this second aspect. This section outlines the main discretized formulations developed to date in the FEM framework, with special attention to those for which isogeometric counterparts have been developed. The latter

will then be the subject of Section 4.

3.1 A brief overview of FEM contact formulations

In the following, a brief overview of the main available FEM contact formulations is presented, paying attention to two important features, namely, the contact patch test performance and the stability. Fulfillement of the contact patch test, first introduced by Taylor and Papadopoulos (1991), ensures the decrease of the discretization error at the contacting surfaces upon mesh refinement. Satisfaction of the so-called inf-sup or Ladyzenskaja-Babuska-Brezzi (LBB) stability condition is an important requirement for mixed formulations, such as those stemming from the contact constraint enforcement with the Lagrange multiplier method. Algorithms that do not fulfil this condition can be solvable if a penalty formulation is used, however may suffer from lack of robustness and significant numerical errors especially for large values of the penalty parameter.

One of the first discretization techniques for large deformation contact problems with non-matching meshes is the node-to-surface (NTS) algorithm (also called node-to-segment in 2D), which is still of pervasive use in commercial finite element codes. Here the contact constraints are enforced between a node of one contact surface (denoted as "slave") and the corresponding surface or edge on the counterpart contact surface (the so-called "master"), which effectively corresponds to collocating the contact integrals at the slave nodes. Early implementations are reported in Hughes et al. (1976, 1977) and Hallquist (1979), and have been extended to more general cases in Bathe and Chaudhary (1985), Hallquist et al. (1985), Wriggers and Simo (1985), Benson and Hallquist (1990), Wriggers et al. (1990), and Papadopoulos and Taylor (1992); see also the review in Zavarise and De Lorenzis (2009a). Obviously, an active set strategy is needed so that only the contributions of slave nodes with a closed gap (i.e. active contact) are included.

While simple and computationally inexpensive, the NTS formulation is unable to satisfy the contact patch test. As shown by Zavarise and De Lorenzis (2009b), this stems from the fact that within this collocated approach the contact pressures are transferred from the slave to the master surface

in the form of concentrated forces at the slave nodes, which leads to violation of the balance of moments at the element level. Attempts to restore local equilibrium (such as in El-Abbasi and Bathe 2001 and Zavarise and De Lorenzis 2009b in a 2D setting) effectively go in the direction of transforming the NTS into a segment-to-segment approach. Note that this local moment imbalance is also one reason why the NTS approach is generally used in conjunction with linear elements (Crisfield 2000). Because of the non-uniform distribution of nodal forces associated with higher order shape functions in presence of a uniform stress field, fulfilment of the patch test is even more difficult with higher order discretizations, which may lead to unnatural distortion of the mesh close to the contacting surfaces.

The NTS algorithm can be proved to be LBB stable (El-Abbasi and Bathe 2001), regardless of whether the finer or the coarser of the two contacting meshes is treated as slave. Its two-pass version, whereby the contact contribution to the weak form is evaluated and incorporated twice while switching the roles of slave and master surfaces, passes the contact patch test but is overconstrained and therefore LBB-unstable. The two-pass version has been developed to alleviate a further drawback of the NTS formulation, i.e. the strong dependency of results on the discretization and on the choice of the slave body due to the biased role of the slave and master surfaces.

Finally, it is worth noting that, in nodal constraint approaches, recovery of the contact traction is not trivial, since this traction is not included explicitly in the formulation but reconstructed after the analysis. This is done e.g. with the so-called tributary area approach, whereby a contact force generated by a constraint is divided by a tributary area to provide a contact traction at that node. The accuracy of the resulting contact pressures is however open to question.

Due to the drawbacks of NTS formulations, several other methods have been developed, where the contact integral is no longer collocated at the slave nodes and the contact constraints are enforced in an integral manner. Early methods of this type are often referred to as surface-to-surface (STS) approaches (or segment-to-segment in 2D). A perturbed Lagrangian formulation first introducing integration over contact segments in 2D was proposed by Simo et al. (1985). Here a piecewise constant approximation of the contact pressure, discontinuous across contact segments, leads to

the enforcement of the contact constraints in an average sense on each contact segment. Further segment-to-segment approaches were proposed by Papadopoulos and Taylor (1992) using quadratic elements in 2D, Papadopoulos and Taylor (1993) using bilinear elements in 3D, and Zavarise and Wriggers (1998) and El Abbasi and Bathe (2001) using 2D linear elements. These approaches typically employ the so-called intermediate contact surfaces, over which contact quantities can be defined and discretized, and adopt mixed methods with the contact pressure as the second field variable, so that a well-defined traction distribution is obtained with no need for *ad-hoc* post-processing schemes.

STS formulations pass the contact patch test thanks to the appropriate definition of intermediate surface segments. However, most of them do not fulfil the LBB stability condition (El-Abbasi and Bathe 2001). Very similar characteristics are exhibited by more recently developed formulations based on the enforcement of the contact constraints at an arbitrary number of contact quadrature points located along the contact surface (Fischer and Wriggers 2005, 2006). In other words, the contact contribution to the weak form is here integrated in a straightforward fashion by locating a predetermined number of Gauss-Legendre quadrature points on each element of the slave contact surface. Obviously, only the contributions of quadrature points with a closed gap (i.e. active contact) are included. In the following, this approach will be denoted as Gauss-point-to-surface (GPTS). Note that in this case the patch test is satisfied only up to within the integration error, as no intermediate surface is introduced and therefore no segmentation for the evaluation of the contact integral is performed. This makes the approach particularly simple to implement. Another advantage of this formulation is that the contact surface is qualitatively well captured even with a low number of elements, unlike in the alternative formulations. This formulation was first proposed for 2D linear and quadratic elements. Later, Franke et al. (2010, 2011) adopted a similar approach using higher order hierarchical shape functions (see Section 2.1.1) and describing the (undeformed) circular geometry of the Hertz contact example exactly with the blending functions method. Their focus was on the use of adaptive mesh refinement and node relocation so as to accurately capture the boundary between contact and no-contact regions and thus avoid spurious oscillations of the

contact pressures at this boundary. Further considerations on this aspect will be reported in Section 4.5.

Papadopoulos et al. (1995) proposed an alternative GPTS formulation, whereby two loops are performed treating each surface alternatively as slave and master. The same formulation was recovered from a very general framework based on surface potentials by Sauer and De Lorenzis (2013), who denoted the approach as "two half-pass formulation" (hereafter GPTS-2hp), as opposed to the classical GPTS procedure termed "full-pass". In each loop ("half-pass"), the contact tractions are computed only on the surface currently treated as slave. Therefore, no transfer of tractions to the master side is needed. Local equilibrium at the surfaces is not enforced *a priori* but was shown to be recovered with high accuracy. The advantages of the two-half pass approach are the unbiased treatment of both surfaces, as well as an increased degree of robustness observed in the numerical computations (Sauer and De Lorenzis 2013). The GPTS-2hp passes the contact patch test to machine precision but is clearly LBB-unstable.

A further improvement has been more recently introduced with the advent of the so-called mortar methods, originally developed as an abstract approach for domain decomposition (Bernardi et al. 1993, 1994). Contact discretizations falling within this framework are characterized by the enforcement of the contact constraints in a weak sense. With this respect, they are similar to STS approaches, however their strength lies in the rigorous mathematical background, which allows a variationally consistent treatment of non-penetration and frictional sliding conditions, and which guarantees optimal convergence rates. In a sense, mortar methods deliver a form of intrinsic algorithmic smoothing through their non-local enforcement of the contact constraints. Early applications of mortar finite element methods for contact mechanics can be found in Belgacem et al. (1998), Belgacem (2000), Hild (2000), McDewitt and Laursen (2000), and Wohlmuth and Krause (2003) among others. Extensions and further developments for large deformation problems can be found e.g. in Yang et al. (2005), Puso and Laursen (2004), Hesch and Betsch (2009), and Tur et al. (2012).

Within Lagrange multiplier formulations, the so-called dual shape functions (Wohlmuth 2000,

2001) have been proposed to discretise the Lagrange multiplier space, which enables the condensation of the multipliers without compromising the optimality of the method. The resulting algorithm, presented in Hüeber and Wohlmuth (2005) for small deformation contact, fulfills the non-penetration condition exactly but, in contrast to standard Lagrange multiplier formulations, does not increase the size of the global problem. In Hartmann et al. (2007) and Hartmann and Ramm (2008) this approach was extended to the kinematically non-linear setting. The consistent linearisation of the contact terms was first given in Popp et al. (2009), whereas a correction for the consistent treatment of boundaries was presented in Cichosz and Bischoff (2011).

Mortar methods simultaneously satisfy patch test and LBB stability requirements (Puso et al. 2008, Hesch and Betsch 2009, Hüeber and Wohlmuth 2009). Their only drawback with respect to the previously reviewed formulations is the higher computational cost, mainly stemming from the computation of the so-called mortar integrals. Since some of these integrals contain the product of shape functions defined on slave and master bodies, the need arises for the introduction of an intermediate contact surface (such as in STS algorithms) and for segmentation techniques, which however enable exact integration only for linear shape functions in 2D. Segmentation is computationally expensive and leads to a very complicated consistent linearization within Newton-Raphson iterative procedures (see e.g. Puso et al. 2008). The alternative of a simplified integration with no segmentation has been pursued by e.g. Tur et al. (2012). For an extensive review of mortar methods for contact problems in FEM see the paper by Popp and Wall in this special issue.

3.2 Issues stemming from C^0 continuity and contact smoothing techniques

In this section we summarize the main issues raised by C^0 continuity within the contact formulations reviewed in the previous section. These are of interest for the purpose of the present review, as they are naturally solved by the isogeometric parameterizations. We also review the main techniques adopted in the conventional FEM setting to alleviate the issue of non-smoothness; see also

Laursen (2002) and Wriggers (2006) for a more detailed overview.

3.2.1 Issues stemming from C^0 continuity

Within the NTS approach, the identification of the master surface or edge associated to a given slave node is performed through closest-point (i.e., normal) projection and thus requires the definition of the normal to the master surface. Undefined or non-uniquely defined normals at the inter-element boundaries as a result of the C^0 continuity of the discretization lead to pathological cases which require special treatments even in a 2D setting (Heegaard and Curnier 1993, Zavarise and De Lorenzis 2009a). In the simplest case, averaging normals between adjacent elements is carried out (Papadopoulos and Taylor 1992, Wang and Nakamachi 1999). More refined treatments introduce a continuous change of the normal vector, or weighted projections of a slave node onto more than one master segment (Liu et al. 1999, Zavarise and De Lorenzis 2009a). In 3D, the need arises for special algorithmic treatments tackling the node-to-edge and the node-to-node subcases beside the standard, well-defined NTS projection cases (Bandeira et al. 2004). Even with incorporation of these special treatments, numerical instabilities may occur, especially for applications involving large sliding, due the non-smooth variation of the contact kinematic and kinetic variables as a slave node slides over subsequent master facets. The resulting abrupt change in the direction of the contact forces may generate unphysical oscillations in the results as well as serious iterative convergence problems and even failure of the analysis.

Pathological projection cases can obviously also occur within GPTS and GPTS-2hp algorithms, where the slave contact quadrature points rather than the slave nodes are projected. The issues are the same as for the NTS approach and can be addressed with the same techniques. Within mortar methods, the "non-local" normal gap evaluated at each slave node is expressed in terms of a nodal normal, whose definition is a crucial ingredient of the formulation as it also influences the way the segmentation procedure is conducted. Here most authors (see e.g. Puso and Laursen 2004, Yang et al. 2005, Puso et al. 2008, Popp et al. 2009) introduce a continuous normal field, which interpolates unique normals at each slave node computed from the average or the

weighted average of the normals to the surfaces surrounding the node. Accordingly, also unique unit tangential vectors are defined. Normal averaging obviously also enters the linearization of the algorithm, and contributes significantly to its complication.

Finally, the C^0 continuity of the parameterization also affects the way frictional evolution equations should be integrated as a node (or a contact quadrature point) slides across element boundaries. The general definition of the tangential slip increment based on the increments of the parametric projections only holds for globally C^1 continuous parameterizations, so that alternative choices must be performed when only C^0 continuity is available (Lengiewicz et al. 2010).

3.2.2 Contact smoothing techniques

In order to alleviate the issues stemming from the C^0 continuity of the discretized contact surfaces, various surface smoothing techniques for 2D and 3D deformable solids in contact have been proposed. These techniques include Hermite (Pietrzak and Curnier 1999, Taylor and Wriggers 1999, Padmanabhan and Laursen 2001), Bézier (Wriggers et al. 2001, Krstulovic-Opara et al. 2002, Lengiewicz et al. 2010), and B-spline interpolations (Padmanabhan and Laursen 2001), Gregory patches (Puso and Laursen 2002, Lengiewicz et al. 2010), subdivision surfaces (Stadler et al. 2003), and NURBS (Landon et al. 2009). For the special case of the contact of a body with a rigid obstacle, various C^1 continuous surfaces can be defined directly from CAGD models of the rigid obstacle, such as in Hansson and Klarbring (1990) and Heege and Alart (1996).

Smoothing procedures generally improve the performance of the contact algorithms by enhancing the continuity of the contact master surface, in order to enable a unique definition of the normal and tangent vector fields, whereas they leave the geometrical smoothness of the slave surface unaltered. This leads to a C^1 or even C^2 continuous representation of the master surface. C^2 continuity is not needed for a smooth normal field but is important in the dynamic setting, where accelerations are discontinuous at the inter-element boundaries if the interpolation is only C^1 continuous (Wriggers 2006).

These procedures lead in general to a more robust behavior of the iterative solution algorithms for contact, since the normal and tangent fields are continuous and thus the issues highlighted in Section 3.2.1 are solved. However, the design of a smoothed master surface in addition to the existing finite element mesh, especially in 3D cases, is far from trivial. Moreover the relationship between real and smoothed geometry needs to be linearized for implicit calculations. Thus smoothing leads to additional complications in the implementation and data management, and can in some cases even compromise the banded structure of the stiffness matrix (Padmanabhan and Laursen 2001).

Obviously, smoothing procedures do not increase the order of spatial convergence since the higher order approximations involve only the surface but not the bulk behavior of the solids. In addition, due to the interaction of the bulk and surface discretizations in determining the smoothness of the traction history curves for large deformation and large sliding problems, the observed improvement in the quality of the contact response may be limited by the fact that the higher order approximation does not involve the bulk behavior of the solid.

The approach by Konyukhov and Schweizerhof (2009) can be considered as a smoothing technique as well. Therein, a single layer of higher order finite elements on the contact surface is combined with a mesh with linear shape functions in the interior of the contacting bodies. In the contact layer, the covariant contact description is used in combination with higher order finite elements with a hierarchical enrichment of the shape functions space, which leads to the exact representation of the contact boundaries by the blending function method (see also Section 2.1.1). Computation of the classical Hertz contact problem showed that oscillations can occur if the contact zone is located inside the master contact segment, as also obtained by Franke et al. (2010, 2011) (see Section 3.1). In such cases, the reduction of the polynomial order together with under-integration was found to improve the results, while not representing a general method. The oscillations stem from the inability of the shape functions to approximate contact pressures featuring non-smoothness within an element (a master segment), see also Section 4.5.

Also in Corbett and Sauer (accepted) contact smoothing is performed by a superficial layer of elements with increased degree and smoothness combined with linear elements in the bulk domain.

Unlike in previous surface enriching techniques by the same group using Hermite or Lagrange interpolations (Sauer 2013), here the formulation of the surface enriched elements is based on IGA. Compared with full IGA formulations, the approach has the advantage of a lower computational cost. However, the low-degree interpolation of the bulk obviously prevents a higher order spatial convergence rate. Due to the use of an isoparametric approach, this method can be considered intermediate between geometry enrichment of the surface layer and fully isogeometric implementations.

Finally, an approach for time integration of frictional evolution equations capable of solving non-smoothness issues without introducing a geometry smoothing was proposed by Agelet de Saracibar (1995). Time integration of frictional tractions is performed by introducing a new assumed slip path parameterization, which is defined independently of the local surface finite element parametrization. The assumed slip path can be viewed as an approximation to the geodesic passing through the initial and final points of each incremental slip path. This eliminates the problems associated with large slip motions, whereby a full incremental slip path does not lie within a single surface element.

4 Isogeometric contact formulations

In this section, we first analyze the main aspects shared by all isogeometric contact formulations that differentiate them from their finite element counterparts. Clearly, these aspects are linked to the properties of the basis functions and to the specific features of the isogeometric setting. Subsequently, we review the isogeometric contact formulations available thus far. Here it is observed that some aspects inherent to the contact formulations themselves, such as patch test performance, stability and computational efficiency, do not change when passing from the FEM to the IGA setting. A summary of FEM and IGA contact formulations is reported in Table 2.

4.1 Aspects common to all isogeometric contact formulations

Geometry and displacement smoothness. A natural way of retaining the advantages of surface smoothing while avoiding the drawbacks mentioned in Section 3.2 is to adopt a parameterization of both the geometry and the displacement field based on NURBS rather than on Lagrange polynomials. Note that, within a large deformation contact setting, smoothness of the geometry alone is not sufficient as the contact forces are computed in the deformed configuration. For this reason, p-FEM approaches with blending functions representing the geometry exactly do not perform as well as IGA (see also Section 4.5). With higher-order IGA basis functions (of at least second order), controllable smoothness is naturally achieved. This straightfowardly eliminates all pathological cases mentioned in Section 3.2 and thus also the need for the corresponding special treatments.

Obviously, only the pathologies induced by the discretization are eliminated, whereas C^0 features such as edges and corners embedded in the exact geometry still need to be dealt with. One option to deal with such features is the use of ad-hoc techniques similar to those used in FEM. An alternative option was proposed by Lu (2011). The premise is that NURBS admit sharp corners through repeated knots, in particular, a degree-k NURBS will feature a cusp at one location if the corresponding interior knot has a multiplicity of k. Thus, a sharp corner can be smoothened by slightly perturbing the repeated knot. Since the control points are unchanged and due to the convex hull property (Section 2), the perturbed curve remains inside the convex polygon defined by the control points. The smoothened curve is at least C^1 continuous, thus closest-point projection algorithms can be used everywhere.

Another situation where C^0 continuity is obtained within IGA is at junctions between different patches. Cases where these junctions form edges and corners may be dealt with exactly as C^0 features in the real geometry. On the other hand, in cases where the real geometry is smooth and C^0 continuity is an artifact of the discretization, C^1 continuity can be explicitly enforced through suitable relationships between the displacements of adjacent control points (Kiendl et al. 2009). The conversion of the NURBS multi-patch model to a single T-spline model is perhaps a more

compelling option (Sederberg et al. 2003).

In the frictional setting, the higher global continuity of the parameterization also permits a straightforward integration of the frictional evolution equations, eliminating the need to keep track of the sliding of a point across element boundaries as well as the need for complicated assumed-path procedures such as the one mentioned in Section 3.2.2.

Patch-wise contact search. In the FEM setting, the contact detection (or local contact search) is conducted essentially element-wise. Each point (node or contact quadrature point) on the slave surface is associated with nearby elements of the master surface with which the point is likely to come into contact and the closest-point projection is limited to these elements. In the large deformation setting, the relative positions of the two surfaces may change significantly and thus the neighbour list needs to be updated as the solution proceeds. As described in Section 2, in the IGA multi-patch framework the parameterization is global for each patch and thus contact detection is carried out on the patch level. In most academic examples, but even for many practical applications, a contact surface can be described by a single patch, hence the bookkeeping task is greatly reduced or even eliminated. Typically, the closest point projection is solved using Newton's method. For a contact surface consisting of multiple patches, this iterative search may land on a patch edge, in which case a patch-switching mechanism needs to be implemented.

Note that the performance of Newton's method is quite sensitive to the initial guess of the projection point, especially for cases in which the second derivative is not continuous. If the initial guess is far from the actual solution, indefinite oscillation between two results may spoil the projection. In such cases, alternative methods such as the bisection method may be used successfully. A possible strategy to start from a sensible initial guess would be to find the closest physical location among the maps of the knot vector entries, and use this as initial guess for the Newton-Raphson iterative procedure. Within a patch, C^2 continuity, which can be attained by cubic NURBS, may prove beneficial.

4.2 Point collocation approaches: the isogeometric NTS

In the isogeometric counterpart of the NTS approach, the contact contribution to the weak form needs to be collocated at appropriate physical points. However, the question where to collocate the contact integrals is not as trivial as in FEM, as the counterparts of the nodes, i.e. the control points, are not necessarily part of the geometry due to the non-interpolatory nature of the basis functions. The most natural option would be to collocate the contact integrals at the physical points associated with the unique knot entries of the NURBS parameterization, i.e. at the vertices of the Bézier elements on the slave surface. However, as unique knot entries are generally fewer than the number of control points, this choice would lead to the number of contact constraints being less than the number of degrees of freedom associated with the slave surface, hence the contact formulation would be underconstrained. A better option, pursued by Matzen et al. (2013) in the 2D frictionless setting, is collocation of the contact integrals at a set of physical points in one-to-one correspondence with the control points associated to the surface. Such sets are e.g. the Greville, Demko or Botella abscissae. Matzen et al. (2013) focused on Botella and Greville abscissae whose locations are obtained straigthforwardly, whereas Demko abscissae have to be computed by a complex iterative algorithm. A convergence study of the Hertzian problem showed that for a contact area near the patch boundary Greville points yield slightly better results.

A different approach was adopted by Benson et al. (2010a,b) within the commercial code LS-DYNA (Hallquist 2006). Here the geometry of the contacting NURBS surfaces is approximated using bilinear quadrilateral interpolation elements so that the existing FEM contact formulations in LS-DYNA are immediately accessible. Each Bézier element may be approximated by one or more interpolation elements, depending on the desired accuracy in the solution of the contact problem. While the slave surface is always approximated with interpolation elements, the master surface may either be approximated or taken as the actual NURBS surface. In the latter case a nonlinear closest-point projection procedure is needed, and a coarse search on the interpolated elements is used to generate a reasonable initial guess. The contact formulation is based on the single-surface algorithm by Benson and Hallquist (1990), which corresponds to a two-pass NTS

formulation combined with an efficient contact search scheme.

The isogeometric NTS formulation preserves the simplicity, but also the main typical disadvantages of an NTS algorithm. Perhaps the most notable of these is the inability to pass the contact patch test. Moreover, the single-pass algorithm (such as in Matzen et al. 2013) suffers from a strong dependency of results on the discretization and on the choice of slave and master surfaces, whereas the double-pass version (such as in Benson et al. 2010a,b) is overconstrained. However, all disadvantages emanating from the non-smooth discretization are naturally avoided, so that the robustness and the overall performance appear far superior to those of NTS models in conventional FEM.

As mentioned in Section 3.1, recovery of contact pressures from an NTS approach is not trivial, and especially so when higher order basis functions are used, therefore Matzen et al. (2013) examined two different methods for obtaining stress distributions from the discrete values of the Lagrange multipliers. In the first approach the contact stress is computed by dividing the contact force at each control point by a tributary length. The second approach is based on the inversion of the standard concept to compute discrete (consistent) nodal forces from distributed loads. Both methods are based on the same input values, namely discrete contact forces at the control points of the basis functions along the contact zone. Hence the Lagrange multipliers need to be first distributed from the collocation points (where they are computed) to the control points. The contribution of the Lagrange multiplier at one collocation point to the contact force at a given control point is computed from its value multiplied by the value of the basis function corresponding to the control point evaluated at the collocation point. The discrete force at the control point is thus the sum of those contributions. Both methods converge with increasing number of degrees of freedom to the analytical solution (for the Hertz example). However, the first method provides a piece-wise constant stress approximation which is rather crude considering that a higher order displacement solution is available. In the second method, independently of the mesh, the numerical solution displays an oscillating behavior with non-physical tensile contact stresses. The oscillations become more localized at the end of the active contact region as the mesh is refined. The authors

attributed this behavior to the inability of high-continuity basis functions to capture the C^0 continuity of the exact contact pressure distribution at the boundary between contact and no-contact regions, similar to what observed by Konyukhov and Schweizerhof (2009) and Franke et al. (2010, 2011) (Section 3.1). They thus successfully evaluated a knot relocation and repetition procedure, similar to the node-relocation strategy used by Franke et al. (2010, 2011) (see also Section 3.1), to lower the continuity at the desired location and eliminate the oscillations. However, a different recovery procedure for the contact pressures used in other IGA contact formulations (see Section 4.5) will be shown to eliminate oscillatory behavior completely in the same Hertz contact example.

Finally, the results of a classical ironing problem show that the NTS approach with NURBS basis functions is able to produce nearly the same results, in terms of magnitude of the oscillations in the traction histories, of a significantly more complex mortar approach with linear basis functions, whereas for the same example with Lagrange basis functions no convergence is achieved. In other words, the higher smoothness of the basis functions combined with the simplest contact algorithm is able to attain the same quality of the global response obtained through the algorithmic smoothing of the more sophisticated mortar method.

4.3 The isogeometric GPTS and GPTS-2hp

The isogeometric counterpart of the GPTS formulation, such as its parent version, is based on the direct integration of the contact contribution to the weak form. Contact Gauss-Legendre quadrature points are situated at predetermined locations along the slave contact surface and the constraints are enforced at all these locations. This approach was termed the "knot-to-surface" algorithm in Temizer et al. (2011), however the contact constraints enforcement does not take place at the physical location of the knot vector entries, which is the reason for the alternate terminology adopted herein. This formulation was demonstrated in combination with the penalty method in Lu (2011) and Temizer et al. (2011) for 2D and 3D frictionless contact and was extended to the 2D frictional setting in De Lorenzis et al. (2012), where the approach was denoted as "non-mortar."

Temizer et al. (2011) formulated and tested the extension to thermomechanical contact. Lu (2011) also evaluated the GPTS-2hp formulation, as well as a two-pass version (denoted subsequently as GPTS-2p), whereby the contact integral was computed twice, switching the role of slave and master surfaces, but multiplied each time by 0.5. More recently, the GPTS algorithm was adopted in a 2D and 3D frictionless setting by Dimitri et al. (2014) in combination with T-spline basis functions to demonstrate the advantages of local refinement.

As its FEM counterpart, the GPTS formulation in the isogeometric setting is characterized by a remarkable simplicity of formulation and implementation, as well as by the possibility to obtain qualitatively good results for very coarse meshes. Compared to the more sophisticated mortar-based approaches, the algorithm is also computationally inexpensive as no quantities such as mortar integrals are involved. The patch test behavior was demonstrated by Lu (2011). As already noted for the FEM case, the GPTS-2hp was able to pass the contact patch test to machine precision, whereas the GPTS and GPTS-2p accuracy was limited by the integration error. Temizer et al. (2011) and De Lorenzis et al. (2011) showed that the overconstrained nature of the GPTS formulation, as for standard Lagrange discretizations, typically leads to oscillatory tractions for the Hertz problem, with oscillations of increasing magnitude as the penalty parameter is increased. These oscillations were particularly significant for the frictional Hertz example in De Lorenzis et al. (2011), due to the independent computations of the slip increments and the associated contact tangential tractions at each contact quadrature point. In Dimitri et al. (2014), the oscillations were alleviated through a smoothing post-processing scheme (Sauer 2013). The issue of overconstraining for the GPTS-2hp, although with NURBS-enriched contact elements rather than within a full IGA setting, was analyzed more thoroughly by Sauer and De Lorenzis (submitted), where it was shown that the formulation remained stable if the penalty parameter was increased along with the mesh density, and once again smooth post-processed contact pressures in both the normal and the tangential directions were obtained.

In the cited references, the direct comparisons between IGA and FEM results was quite limited, as the focus was placed on mortar methods, but the comparisons always favored the IGA dis-

cretizations. In Dimitri et al. (2014) a convergence study conducted for T-splines showed similar orders of convergence to uniform and non-uniform equal degree NURBS discretizations. Despite the absence of error estimation criteria to guide the local T-spline refinement, the T-spline error curve was shown to lie below all the NURBS curves, thus demonstrating the superior accuracy of T-splines for a given number of degrees of freedom. The authors also reported a 3D example with a complex realistic geometry produced directly in a CAD environment, without intermediate mesh generation, feature removal, or geometry clean-up steps.

4.4 The isogeometric mortar formulation

The isogeometric mortar contact formulation, such as its FEM counterpart, is not a collocation approach such as the NTS approach because the weak form of the contact constraints is evaluated by numerical integration. On the other hand, the contact constraints are not enforced at each contact quadrature point on the slave surface such as in the GPTS approach, but rather "projected" to the degrees of freedom of the slave surface, so that the right number of constraints is obtained. For example in a frictionless setting, "mortar projected" normal gap and normal pressure are computed at each control point of the slave surface and these have to satisfy the contact constraints. Due to the non-interpolatory nature of the NURBS basis functions, the slave control points in general do not lie on the physical slave surface, therefore the mortar contact constraints do not have the immediate physical meaning that they possess in the FEM setting. This however does not affect the consistency nor the performance of the algorithm.

Mortar isogeometric contact formulations have been presented by Temizer et al. (2011) and Kim and Youn (2012) in the 2D frictionless setting, by De Lorenzis et al. (2011) for 2D friction, and extended to 3D by De Lorenzis et al. (2012) and Temizer et al. (2012) in the frictionless and frictional settings, respectively. In these approaches the contact constraints were enforced with the penalty (Temizer et al. 2011, De Lorenzis et al. 2011), Lagrange multiplier (Kim and Youn 2012), and augmented Lagrangian methods either with Uzawa augmentations (Temizer et al. 2012) or

with the formulation proposed by Alart and Curnier (De Lorenzis et al. 2012).

As in FEM, isogeometric mortar contact formulations satisfy both the patch test and the LBB stability requirements. The patch test performance has been demonstrated by Kim and Youn (2012), whereas the implications of stability have been discussed by Temizer et al. (2011) and De Lorenzis et al. (2011). They showed the absence of oscillatory behavior in the contact pressures as the penalty parameter was increased, in contrast to the results of the GPTS formulation.

The mortar contact formulation was shown by Temizer et al. (2011, 2012) and De Lorenzis et al. (2011, 2012) to deliver two categories of advantages over its FEM counterpart. First, the quality of the local results, i.e. of the contact pressures (e.g. in the classical Hertz problem), was found to be superior to that achieved with Lagrange discretization. The contact pressure distributions stemming from the NURBS parameterizations were always non-negative, were practically insensitive to changes in the interpolation order, and improved monotonically as the mesh resolution increased. The respective distributions obtained from Lagrange parameterizations were highly sensitive to the interpolation order, displayed significant spurious oscillations, and in some cases attained large non-physical negative values. It is important to note that, in these contributions, the pressure distributions along the contact surface were reconstructed by interpolation of the control point values using NURBS (or Lagrange) basis functions. Results obtained with this same reconstruction techniques will be presented in Section 4.5. Second, the quality of the global results, i.e. of force-displacement or moment-rotation histories was also found to improve. In large frictional sliding problems the time histories of the tractions obtained from the NURBS discretizations were remarkably smooth and improved in quality with increasing order of the parameterization. Conversely, the curves obtained from Lagrange parameterizations displayed irregular oscillations whose magnitude increased with the interpolation order and which in some cases even prevented convergence.

The only negative side of mortar approaches, such as for FEM, is the significant computational cost connected to the computation and storage of the mortar integrals. In particular, a crucial aspect is the integration of the "mixed" mortar integrals (i.e. those containing the products of basis

functions related to the slave and master discretized surfaces). In the above cited contributions, integration was performed with the simplified technique mentioned in Section 3.1 (used in the FEM setting by Tur et al. 2012 among others). With this method, no segmentation of the contacting surfaces is performed. Rather, quadrature points are projected from the slave to the master surface and the mixed mortar integrals are computed taking the values at the slave quadrature points and those at their projection points for the basis functions related to the slave and master surfaces, respectively. The simplicity of this approach goes at the expenses of the robustness, especially for large sliding cases or for cases where the slave surface is in intermittent or partial contact. A partial improvement was proposed by Kim and Youn (2012) in the 2D setting. In their approach, each slave surface element in partial contact is divided through knot insertion into its active and inactive portions, and an iterative procedure based on the bisection method is used to identify the boundary of the active region. The newly inserted knots are used only temporarily for integration purposes and later eliminated. However, this method does not solve the aforementioned issue, as even integration on slave segments in fully active contact would require segmentation due to the non-matching discretizations of the two surfaces. To date, no isogeometric counterparts of the mortar contact formulation including computation of the mortar integrals via segmentation is available. As mentioned earlier, segmentation procedures for FEM lead to an exact evaluation of the mortar integrals only in the 2D case with linear shape functions. Obviously, finding efficient and accurate segmentation techniques for higher order and higher smoothness shape functions would not be a trivial task. Also, linearization of the ensuing contact formulation would introduce a remarkable degree of complication as well as computational cost. On the other hand, probably an even more robust performance of the resulting algorithm would be achieved, especially for cases with extreme deformations and very large sliding.

Finally, it is worth noting that an isogeometric counterpart of the dual mortar approach (Wohlmuth 2000, 2001) has not yet been developed. While being certainly not trivial to derive, such an approach has the potential to greatly enhance the computational efficiency of mortar-based isogeometric methods for contact problems.

4.5 The Hertz contact problem revisited

Hereafter, the classical Hertz frictionless contact problem between a cylinder (slave) and a rigid plane (master) is revisited in order to highlight the role played by the properties of the basis functions on the results, and to put forth some observations on the reconstruction of the contact pressures. The cylinder has radius $R = 1$ and its material is linearly elastic with Young's modulus $E = 1$ and Poisson's ratio $\nu = 0.3$. Only a quarter of the geometry is considered, see Figure 2. The cylinder is loaded with a vertical force $P = 0.002$ applied as distributed load on the upper surface. The analytical solution for this problem is well known and yields $p_0 = 0.02645$ and $a = 0.048$ for this value of applied force, p_0 and a being, respectively, the maximum normal pressure and the half-width of the contact area. Different meshes are considered to evaluate the effect of mesh refinement. In all cases, the mesh is refined close to the contact region using non-uniform knot vectors, and the chosen amount of redistribution of the knot vector entries is such that 80% of the elements are located within 10% of the total length of the knot vector in both parametric directions.

Computations are performed with the mortar method in the implementation of De Lorenzis et al. (2011, 2012). Since the master body is rigid, the use of the simplified integration scheme with no segmentation does not play any role on results. The penalty method is used with a penalty parameter fixed at 10^3.

The same computations are repeated with four categories of shape functions (see also Section 2):

- conventional Lagrange shape functions (L^p), featuring C^0 inter-element continuity and describing the circular geometry approximately;

- hierarchical Lagrange shape functions using the blending function method (L_b^p), featuring C^0 interelement continuity for the unknown displacement field and describing the circular geometry exactly;

- Bernstein shape functions (B^p), featuring C^0 inter-element continuity and describing the circular geometry exactly, with the additional non-negativity and convex hull/variation diminishing

properties;

- NURBS shape functions (N^p), featuring C^{p-1} inter-element continuity and describing the circular geometry exactly, with the additional non-negativity and convex hull/variation diminishing properties.

The Bézier interpolation (based on Bernstein shape functions) was obtained from the NURBS one by means of so-called Bézier extraction, which consists in repeatedly duplicating all interior knots in the knot vectors until their multiplicity equals the order p. The resulting interpolation is thus C^0 continuous and interpolatory such as the Lagrange one, however possesses the additional non-negativity and convex hull/variation diminishing properties. Note that, starting from the same knot vectors, discretizations obtained throught Bézier extraction are obviously finer than the parent NURBS ones. Herein, discretizations with the same final number of control points are considered for a more meaningful comparison.

Results are reported in Figures 3 to 10, where the dimensionless contact pressure p/p_0 is plotted versus the dimensionless coordinate x/a. As in Temizer et al. (2011, 2012) and De Lorenzis et al. (2011, 2012), the pressure distributions along the contact surface are reconstructed by interpolation of the control point values using the same basis functions adopted for the displacement solution.

The comparison between results obtained with L^p and L_b^p functions isolates the role of an exact description of the circular geometry. As the figures show, this factor plays virtually no role in this case. It is perhaps worth recalling that the analytical solution by Hertz was found under the assumption of a small contact area, so that the circular shape is in fact approximated by a parabola. Under conditions where this assumption holds (such as in the present example), the geometry is thus equivalently well approximated by second-order Lagrange and hierarchical basis functions with the blending function method. For basis functions of different orders, the hierarchical basis with blending functions maintains an exact description whereas the Lagrange approximation introduces a geometry deviation from Hertz's assumptions. Nevertheless, there is virtually no difference between results from the two sets of basis functions, probably due to the contact computations being carried out in the deformed configuration.

In both cases, the best results are obtained with linear discretizations, whereas significant oscillations appear in the higher order curves. These stem from the Lagrange basis being interpolatory, and thus oscillatory. Also, due to the possibility of these basis functions to take negative values, the interpolation of the control point pressure values leads in some cases to negative (i.e. tensile) pressures, which are obviously unphysical. This typically occurs at the edge of the contact region whenever it happens to fall within an element. As mentioned earlier, this phenomenon was addressed by Franke et al. (2010, 2011) using adaptive relocation of nodes to let the edge of the contact region coincide with an element boundary.

A subsequent comparison can be carried out between L^p and B^p results. The difference between the two sets of functions consists in the fact that the Bernstein basis functions are non-negative and exhibit the convex hull/variation diminishing property. As a result of the first property, no negative contact pressure values are obtained. Due to the second property, the magnitude of the oscillations is greatly reduced, as the functions are only interpolatory at the element boundaries (where the C^0 continuity is clearly visible) and their values are bounded by the polygon of the control point values. The edge of the contact region is again the least accurate location when the edge does not coincide with an element boundary, however the inability to capture the exact solution does not lead to oscillatory behavior in contrast to what observed in the L^p case.

Further, B^p results can be compared with N^p results. Here the difference between the basis functions consists only in the higher continuity of the N^p basis, which is immediately visible in the curves. The functions are now interpolatory only at the patch boundaries. Obviously, the C^0 exact solution at the edge of the contact region cannot be captured. Note that this would be the case even if this edge happened to coincide with an element boundary. An option to capture the edge accurately would be an adaptive knot relocation procedure (the isogeometric counterpart of the node relocation advocated by Franke et al. 2010, 2011) combined with knot repetition to achieve a local lowering of continuity.

Note that the previous results differ significantly from those presented by Matzen et al. (2013), where for the Hertz problem solved with NURBS basis functions an oscillatory behavior was

obtained at the edge of the contact region, such as seen here for Lagrange basis functions. In our opinion, this is to be attributed to the different procedure used for the reconstruction of the contact pressures. Unlike those in Matzen et al. (2013), results presented in this section are based on interpolation of control point values, and therefore take full advantage of the favorable interpolation properties of Bernstein and NURBS basis functions. This aspect should be taken into account while selecting appropriate pressure reconstruction procedures for general contact algorithms.

The key message of this example is that the higher inter-element continuity is not the only advantage of isogeometric contact formulations. In frictionless cases with no or limited sliding, other properties of the isogeometric basis functions, namely the non-negativity and convex hull/variation diminishing properties, may be as important or even more important than continuity. On the other hand, an exact description of the geometry may have a minor importance in the large-deformation setting. For examples with large sliding and especially in frictional cases, continuity is certainly the key to the better performance of isogeometric contact formulations, for the reasons highlighted in earlier sections and as extensively demonstrated by the cited references.

4.6 A rotating ironing example

As a further demonstration of the capabilities of IGA discretizations in the context of contact, we briefly illustrate a challenging example where large deformations and large sliding take place. The initial discretized geometry is shown in Figure 11a: a deformable indentor (in-plane dimensions 1.0 x 1.0, total height approximately 1.0) is pressed onto a deformable slab (dimensions 3 x 1.5 x 0.75) applying a vertical displacement of -0.75 (including an initial gap between the bodies of approximately 0.05) in 15 time steps. Subsequently, the indentor is simultaneously dragged 1.45 units across the slab and rotated 90 degrees along its centroidal vertical axis in 50 additional time steps. Both materials feature a neo-Hooke elastic behavior based on the strain energy function

$$\Psi = \frac{\mu}{2}\left(\mathrm{tr}\mathbf{C} - 3\right) - \mu \ln J + \frac{\lambda}{4}\left(J^2 - 1 - 2\ln J\right) \tag{18}$$

where the Lamé constants λ and μ correspond to $E = 1$ and $\nu = 0.2$, $\mathbf{C}$ is the right Cauchy-Green deformation tensor, and $J = \det\mathbf{F}$ with $\mathbf{F}$ as the deformation gradient. For the discretization second-order NURBS are used in all parametric directions. Frictionless contact is assumed between the bodies and the contact constraints are enforced with the penalty method, using a normal penalty parameter fixed at 10^2. The example is run with the isogeometric GPTS formulation with 8 x 8 Gauss surface quadrature points.

Figures 11b-h are snapshots of the analysis, including contour plots of the vertical Cauchy stress component, σ_{33}, on the centroidal longitudinal cross-section. The C^1 continuity of the second-order NURBS discretization is the key for the achievement of convergence in this challenging problem, as well as for the remarkable smoothness of the vertical reaction history reported in Figure 12.

4.7 Contact formulation for isogeometric collocation

All the approaches discussed thus far, within both the FEM and the IGA frameworks, are based on the Galerkin method, i.e. on the solution of the weak form of the governing equations including a contact contribution. Recently, an alternative approach denoted as isogeometric collocation is showing a significant potential to significantly enhance the efficiency of isogeometric methods. As opposed to Galerkin formulations, isogeometric collocation is based on the discretization of the strong form of the governing partial differential equations, which is only possible with basis functions of sufficient smoothness such as those used in IGA (Auricchio et al. 2012, Schillinger et al. 2013). As isogeometric collocation methods emerge, contact formulations suitable for this framework are needed to tackle problems involving interactions between multiple bodies with non-conforming discretizations. In De Lorenzis et al. (submitted), such a contact formulation is developed and implemented.

In isogeometric collocation, the discretized governing equations of the elastostatic problem, as well

as the Neumann boundary conditions, are enforced at the appropriate collocation points, whereas the Dirichlet boundary conditions are built into the solution space. Note that the collocation points are typically chosen as the Greville or Demko abscissae of the knot vectors, already mentioned in Section 4.2. These are equal in number to the control points and some are always located on the boundary of the domain. In this setting, the most natural approach to enforce the contact constraints is to treat them as deformation-dependent Neumann boundary conditions on the portion of the boundary in active contact, which may be identified with classical active set strategies.

All the formulations reviewed in Section 3.1, as well as their isogeometric counterparts in Section 4, enforce *a priori* the local pressure equilibrium between the contacting bodies, with the exception of the GPTS-2hp. This is the main reason why these formulations do not fit well into the collocation framework. Should one of the contacting surfaces be chosen as slave, the gap would need to be evaluated and the contact constraints enforced at all collocation points located on the slave surface. The contact traction $\mathbf{t}$ would thus be computed on the slave surface, and due to the *a priori* enforcement of equilibrium the opposite traction $-\mathbf{t}$ would need to be applied to the master surface. However, this transfer would not be obvious to realize for meshes with non-matching location of the collocation points on the contacting surfaces, whereas the same transfer is achieved naturally within a weak formulation in the Galerkin setting.

Conversely, in the GPTS-2hp approach, two loops are performed treating each surface alternatively as slave and master. In each half-pass, the contact tractions are computed only on the surface currently treated as slave. Therefore, no transfer of tractions to the master side is needed. For this reason, the GPTS-2hp formulation is adopted in De Lorenzis et al. (submitted) to address the enforcement of contact constraints within the collocation framework and the resulting formulation is tested using a penalty regularization.

Interestingly, the contact collocation approach passes the contact patch test to machine precision despite its local enforcement of the contact constraints at the collocation points. The reason is that the contact-related equations, being obtained from the collocation of the Neumann boundary conditions in strong form, directly involve contact *pressures*. Conversely, in the NTS approach

where the contact constraints are also enforced locally at the slave nodes (in FEM, see Section 3.1) or at the same collocation points (see Section 4.2), the contact residual contributions are computed in the form of *concentrated forces*, and recovery of the contact pressure distribution from these forces does not lead to satisfaction of the patch test due to the local moment imbalance pointed out in Zavarise and De Lorenzis (2009b).

The contact formulation in the isogeometric collocation setting yields results of very good quality for regular solutions and uniform meshes. In situations with highly non-uniform meshes, the original collocation approach leads to a loss of accuracy in the form of local oscillations near the boundary, which is also observed for the enforcement of standard Neumann boundary conditions. In the case of contact, the oscillations may even spoil the iterative convergence behavior leading to failure of the analysis. The issue is solved by an enhanced collocation scheme, whereby Neumann and contact conditions are written including not only a boundary but also a weighted interior term. This remedy restores accuracy of the results and robustness of the iterative procedure.

4.8 Beam-to-beam contact formulation

Konyukhov and Schweizerhof (2012) presented a geometrically exact theory for contact interactions of 1D manifolds in the 3D space, including edge-to-edge, beam-to-beam, cable-to-edge contact cases. The geometrically exact curve-to-curve contact formulation was combined with various types of approximations, including NURBS-based isogeometric beam elements, and demonstrated through examples dealing with the simulation of knot tying. In the knot tying example, convergence could only be achieved using isogeometric elements, whereas the C^0 continuity of higher order Lagrange elements led to divergence during the first crossing of element boundaries.

5 Domain decomposition approaches, extensions and applications of IGA contact formulations

In this section we briefly review investigations not directly focused on the development of new isogeometric contact formulations, but nevertheless relevant to the topic of contact or to modeling of interfaces with non-matching discretizations in a broader sense.

5.1 Domain decomposition approaches

Hesch and Betsch (2012) presented a mortar method for the coupling of non-conforming discretized sub-domains in nonlinear elasticity, whereby mortar integrals were redefined for the IGA framework. An important feature of the approach was the combined use of Lagrange and NURBS shape functions. This makes it possible to apply IGA in a reasonable fashion and to use Lagrange shape functions if necessary. The authors applied a specific coordinate augmentation technique to achieve an energy–momentum consistent formulation of the constrained mechanical system.

In Reuss et al. (2014), the weak enforcement of interface constraints with Nitsche's method was used as a coupling tool for non-matching trimmed NURBS patches, as well as for the connection of spline discretizations with standard triangular finite element meshes. It was shown that the combination of the Nitsche-based coupling methodology with the finite cell method paves the way for a treatment of trimmed multi-patch NURBS geometries that completely eliminates the need for reparameterization procedures. Also, Nitsche-based coupling was shown to lead to optimal rates of convergence under h-refinement and exponential rates of convergence under p-refinement, and did not introduce error concentrations along the coupling interfaces.

5.2 Extensions

The study of thermomechanical contact with IGA discretizations was initiated by Temizer et al. (2011), where thermoelastic calculations of the contact of a Grosch wheel with a plane rigid

surface were first presented. In Temizer (2013), an isogeometric thermomechanical mortar contact formulation was applied within a computational homogenization framework for boundary layers with microscopically rough surfaces. A two-phase homogenization approach combined with the mortar contact algorithm within IGA was shown to deliver a computational framework of optimal efficiency that can accurately represent the geometry of smooth surface textures.

Dimitri et al. (in press) presented a NURBS- and T-spline-based isogeometric formulation for 2D and 3D interface problems with non-matching meshes encompassing contact and mode-I debonding, based on a generalized version of the GPTS contact algorithm endowed with a cohesive zone model. In the examples, the performance of Lagrange, NURBS and T-spline discretizations was evaluated. In contrast to Lagrange discretizations, the use of NURBS led to very small oscillations whereas T-spline models with the same number of degrees of freedom delivered macroscopically smooth results due to their ability to be locally refined, which led to a better resolution of the fracture process zone in the vicinity of the interface and ahead of the cohesive crack. The proposed formulation, combined with T-spline isogeometric discretizations featuring high inter-element continuity and local refinement ability, was thus shown to be a computationally accurate and efficient technology for the solution of more general interface problems than the pure geometric enforcement of the non-penetration constraints.

5.3 Applications

Due to the analyzed advantages, isogeometric contact formulations have been adopted in a number of recent studies focusing on various applications. In De Lorenzis and Wriggers (2013) computational contact homogenization was conducted to derive a macroscopic effective friction coefficient for rubber as a function of sliding velocity and applied pressure. A central ingredient of the microscale boundary value problem was contact between the rubber sample and a sinusoidally rough surface. The numerical model was developed within the isogeometric framework with a mortar formulation, which was demonstrated to lead to faster spatial convergence in comparison with the

use of conventional linear elements.

Sauer (submitted) presented a liquid membrane formulation suitable to analyze liquid films with special attention to their contact behavior. A comparison between Lagrange and NURBS discretizations demonstrated the better accuracy of IGA. Sauer et al. (submitted) presented a geometrically exact membrane formulation based on curvilinear coordinates and isogeometric finite elements, suitable for both solid and liquid membranes including their contact constraints. The new formulation was illustrated by several examples, considering linear and quadratic Lagrange elements, as well as isogeometric elements based on quadratic NURBS and cubic T-splines. The examples showed large accuracy gains between linear and quadratic Lagrange, and between quadratic Lagrange and isogeometric finite elements. The formulation was successfully applied to liquid droplets, including contact angles and rough surface contact.

Lu and Zheng (2014) developed a NURBS-based continuum approach of cloth simulation, including an explicit formulation for contact/impact. The adopted two step impulse-based algorithm, taken from the available literature, was shown to deal robustly with complicated contact conditions and to recover a constant quasi-static pressure field in a pressure patch test. The contact detection scheme, based on the NTS approach, included self-contact. The Newton iterations for contact detection were reported to suffer from numerical difficulties in the case of complicated geometries, arising from the non-uniqueness of the solution. An accelerated local search was thus introduced to improve the initial guess, based on an auxiliary tessellation mesh obtained by splitting each NURBS element into two triangles. In the simulations, the slave surface was alway parameterized with NURBS while the master surface could be either a NURBS surface (cloth-cloth contact) or a polygon mesh (cloth-object contact where the object is represented by a polygon mesh). Despite the limitations of the approach due to the accuracy and step size issue intrinsic to explicit formulations, the proposed method proved promising as an analysis tool in textile/garment engineering and possibly for computer graphics.

Morganti et al. (in preparation) presented the application of NURBS-based IGA to the model construction and simulation of aortic valve closure. A key ingredient of the model is the description

of contact between the three aortic leaflets during closure of the aortic valve. The mechanics of contact also dictates important measures of the physiological behavior such as the coaptation length. The authors used the contact formulation by Benson et al. (2010a,b) within LS-DYNA. IGA facilitated the development of analysis-suitable patient-specific models and, in the simulations, was capable of attaining the same accuracy as FEM with two orders of magnitude fewer degrees of freedom.

6 Research needs and conclusions

We reviewed the currently available isogeometric contact formulations, placing them into the global context of computational contact mechanics. The advantages of IGA for the solution of challenging contact problems are quite evident, and stem from the favorable properties of isogeometric basis functions, most notably, the higher and controllable continuity at the inter-element boundary achieved for the geometry but also, within an isoparametric approach, for the unknown displacement field, and the convex hull and variation diminishing properties.

These advantages have not yet been fully explored and exploited. A few open issues and possible directions for further research, as directly emerging from the above review, are summarized as follows:

- the efficiency and robustness of isogeometric mortar contact formulations is strongly influenced by the strategy used for the computation and storage of the mortar integrals. The development of accurate and yet efficient integration schemes would thus represent a significant advancement, as would the development of dual mortar formulations for the condensation of the additional degrees of freedom arising in a Lagrange multiplier approach;

- the local refinement capability of T-spline interpolations and the ability to represent a complex geometry of arbitrary topology as a single watertight parameterization have recently been proved to provide significant advantages for contact modeling when compared

to NURBS interpolations. To fully exploit these advantages, error-controlled adaptive refinement procedures are needed. For the same purpose, alternative basis functions such as hierarchical B-splines or isogeometric spline forests could also prove interesting. Moreover, mortar-based contact formulations have never been applied to isogeometric discretizations capable of local refinement;

- the higher smoothness of isogeometric basis functions leads to inaccuracies at the boundaries between contact and no-contact regions, i.e. where the exact solution features C^0 continuity possibly within an element. While not leading to oscillatory behavior (differently from what is observed in FEM), these situations may compromise optimal convergence and could be tackled using ad-hoc strategies such as local lowering of continuity, local knot relocation, and local partition of unity approaches. This issue has not yet been addressed;

- as isogeometric collocation emerges as a competitive technology in computational mechanics, further investigations should be conducted on contact within the collocation framework, where the first steps have recently been taken and have shown very promising results.

Some of these directions are being currently pursued by the authors.

7 Acknowledgments

L. De Lorenzis has received funding for this research from the European Research Council under the European Union's Seventh Framework Programme (FP7/2007-2013) / ERC Grant agreement n° 279439. T.J.R. Hughes was supported by grants from the Office of Naval Research (N00014-08-1-0992), the National Science Foundation (CMMI-01101007), and SINTEF (UTA10-000374) with the University of Texas at Austin.

References

[1] C. Agelet de Saracibar (1997). A new frictional time integration algorithm for large slip multi-body frictional contact problems. Compstruuter Methods in Applied Mechanics and Engineering, 142: 303-334.

[2] P. Alart, A. Curnier (1991). A mixed formulation for frictional contact problems prone to Newton like solution methods. Computer Methods in Applied Mechanics and Engineering, 92: 353-375.

[3] F. Auricchio, L. Beirão da Veiga, T.J.R. Hughes, A. Reali, G. Sangalli (2012). Isogeometric collocation for elastostatics and explicit dynamics. Computer Methods in Applied Mechanics and Engineering, 249–252: 2–14.

[4] A.A. Bandeira, P. Wriggers, P. de Mattos Pimenta (2004). Numerical derivation of contact mechanics interface laws using a finite element approach for large 3D deformation. International Journal for Numerical Methods in Engineering, 59: 173–195.

[5] Y. Bazilevs, V. Calo, J. Cottrell, J.A. Evans, T.J.R. Hughes, S. Lipton, M. Scott, T. Sederberg (2010). Isogeometric analysis using T-splines. Computer Methods in Applied Mechanics and Engineering, 199: 229–263.

[6] K. Bathe, A. Chaudhary (1985). A solution method for planar and axisymmetric contact problems. International Journal for Numerical Methods in Engineering, 21: 65–88.

[7] F. Ben Belgacem, P. Hild, P. Laborde (1998). The mortar finite element method for contact problems. Mathematical and Computer Modelling, 28: 263–271.

[8] F. Ben Belgacem (2000). Numerical simulation of some variational inequalities arisen from unilateral contact problems by the finite element methods. SIAM Journal on Numerical Analysis 37:1198–1216.

[9] D.J. Benson, J.O. Hallquist (1990). A single surface contact algorithm for the postbuckling analysis of shell structures. Computer Methods in Applied Mechanics and Engineering, 78: 141–163.

[10] D.J. Benson, Y. Bazilevs, E. De Luycker, M.C. Hsu, M. Scott, T.J.R. Hughes, T. Belytschko (2010a). A generalized finite element formulation for arbitrary basis functions: From isogeometric analysis to XFEM. International Journal for Numerical Methods in Engineering, 83(6): 765–785.

[11] D.J. Benson, Y. Bazilevs, M.C. Hsu, T.J.R. Hughes (2010b). Isogeometric shell analysis: The Reissner–Mindlin shell. Computer Methods in Applied Mechanics and Engineering, 199: 276–289.

[12] C. Bernardi, Y. Maday, A. Patera (1993). Domain decomposition by the mortar element method. In: H. Kasper, M. Garby (Eds.), Asymptotic and Numerical Methods for Partial Differential Equations with Critical Parameters: Proceedings of the NATO Advanced Research Workshop on Asymptotic-Induced Numerical Methods for Partial Differential Equations, Critical Parameters, and Domain Decomposition, Science Series C, Beaune, Frankreich, NATO, 384: 269–286.

[13] C. Bernardi, Y. Maday, A. Patera (1994). A new nonconforming approach to domain decomposition: the mortar element method. In: H. Brezis, J. Lions (Eds.), Nonlinear Partial Differential Equations and Their Applications, Collége de France Seminar, 12: 13–51.

[14] M.J. Borden, M.A. Scott, J.A. Evans, T.J.R. Hughes (2011). Isogeometric finite element data structures based on Bézier extraction of NURBS. International Journal for Numerical Methods in Engineering, 87:15–47.

[15] T. Cichosz, M. Bischoff (2011). Consistent treatment of boundaries with mortar contact formulations using dual Lagrange multipliers. Computer Methods in Applied Mechanics and Engineering, 200: 1317–1332.

[16] P.W. Christensen, A. Klarbring, J. S. Pang, N. Strömberg (1998). Formulation and comparison of algorithms for frictional contact problems. International Journal for Numerical Methods in Engineering, 42(1): 145–173.

[17] C.J. Corbett, R.A. Sauer (accepted). NURBS-enriched contact finite elements. Computer Methods in Applied Mechanics and Engineering.

[18] J.A. Cottrell, T.J.R. Hughes, Y. Bazilevs (2009). Isogeometric analysis: Towards Integration of CAD and FEA. John Wiley & Sons.

[19] M.A. Crisfield (2000). Re-visiting the contact patch test. International Journal for Numerical Methods in Engineering, 48:435–449.

[20] L. De Lorenzis, I. Temizer, P. Wriggers, G. Zavarise (2011). A large deformation frictional contact formulation using NURBS-based isogeometric analysis. International Journal for Numerical Methods in Engineering, 87(13): 1278-1300.

[21] L. De Lorenzis, P. Wriggers, G. Zavarise (2012). A mortar formulation for 3D large deformation contact using NURBS-based isogeometric analysis and the augmented Lagrangian method. Computational Mechanics, 49(1): 1-20.

[22] L. De Lorenzis, P. Wriggers (2013). Computational homogenization of rubber friction on rough rigid surfaces. Computational Materials Science, 77: 264-280.

[23] L. De Lorenzis, J. A. Evans, T.J.R. Hughes, A. Reali (submitted). Isogeometric collocation: traction boundary conditions and large-deformation contact.

[24] R. Dimitri, L. De Lorenzis, M.A. Scott, P. Wriggers, R.L. Taylor, G. Zavarise (2014). Isogeometric large deformation frictionless contact using T-splines. Computer Methods in Applied Mechanics and Engineering, 269: 394-414.

[25] R. Dimitri, L. De Lorenzis, P. Wriggers, G. Zavarise (accepted). NURBS- and T-spline-based isogeometric cohesive zone modeling of interface debonding, Computational Mechanics.

[26] A. Düster, H. Bröker, E. Rank (2001). The p-version of the finite element method for three-dimensional curved thin walled structures. International Journal for Numerical Methods in Engineering, 52: 673–703.

[27] N. El-Abbasi, K. J. Bathe (2001). Stability and patch test performance of contact discretizations and a new solution algorithm. Computers & Structures, 79: 1473–1486.

[28] A.L. Eterovic, K.J. Bathe (1991). An interface interpolation scheme for quadratic convergence in the finite element analysis of contact problems. In: Computational Methods in Nonlinear Mechanics, Springer-Verlag, Berlin, New York, 703–715.

[29] J.A. Evans, Y. Bazilevs, I. Babuška, T.J.R. Hughes (2009). n-widths, sup-infs, and optimality ratios for the k -version of the isogeometric finite element method. Computer Methods in Applied Mechanics and Engineering, 198(21–26): 1726–1741.

[30] K. A. Fischer, P. Wriggers (2005). Frictionless 2D contact formulations for finite deformations based on the mortar method. Computational Mechanics, 36: 226–244.

[31] K. A. Fischer, P. Wriggers (2006). Mortar based frictional contact formulation for higher order interpolations using the moving friction cone. Computer Methods in Applied Mechanics and Engineering, 2006: 5020–5036.

[32] D. Franke, A. Düster, V. Nübel, E. Rank (2010). A comparison of the h-, p-, hp-, and rp-version of the FEM for the solution of the 2D Hertzian contact problem. Computational Mechanics, 45: 513–522.

[33] D. Franke, E. Rank, A. Düster (2011). Computational contact mechanics based on the rp-version of the finite element method. International Journal of Computational Methods, 8(3): 493–512.

[34] W.J. Gordon, C.A. Hall (1973). Transfinite elementmethods: blending function interpolation over arbitrary curved element domains. Numerical Mathematics, 21:109–129.

[35] D. Großmann, B. Jüttler, H. Schlusnus, J. Barner, A.H. Vuong (2012). Isogeometric simulation of turbine blades for aircraft engines. Computer Aided Geometric Design, 29(7):519–531.

[36] J.O. Hallquist (1979). Nike2D: an implicit, finite deformation, finite element code for analyzing the static and dynamic response of two-dimensional solids. Tech. Rep. UCRL-52678, Lawrence Livermore National Laboratory, University of California, Livermore.

[37] J. Hallquist, G. Goudreau, D. Benson (1985). Sliding interfaces with contact-impact in large-scale Lagrange computations. Computer Methods in Applied Mechanics and Engineering, 51: 107–137.

[38] J. Hallquist (2006). LS-Dyna Theory Manual.

[39] E. Hansson, A. Klarbring (1990). Rigid contact modelled by CAD surface. Engineering Computations, 7: 344–348.

[40] S. Hartmann, S. Brunssen, E. Ramm, B. Wohlmuth (2007). Unilateral non-linear dynamic contact of thin-walled structures using a primal-dual active set strategy. International Journal for Numerical Methods in Engineering, 70: 883–912.

[41] S. Hartmann, E. Ramm (2008). A mortar based contact formulation for non-linear dynamics using dual Lagrange multipliers. Finite Elements in Analysis and Design, 44: 245–258.

[42] J.-H. Heegaard, A. Curnier (1993). An augmented Lagrange method for discrete largeslip contact problems. International Journal for Numerical Methods in Engineering, 36: 569–593.

[43] A. Heege, P. Alart (1996). A frictional contact element for strongly curved contact problems. International Journal for Numerical Methods in Engineering 39: 165–184.

[44] C. Hesch, P. Betsch (2009). A mortar method for energy-momentum conserving schemes in frictionless dynamic contact problems. International Journal for Numerical Methods in Engineering, 77: 1468–1500.

[45] C. Hesch, P. Betsch (2012). Isogeometric analysis and domain decomposition methods. Computer Methods in Applied Mechanics and Engineering, 213-216: 104-112.

[46] P. Hild (2000). Numerical implementation of two nonconforming finite element methods for unilateral contact. Computer Methods in Applied Mechanics and Engineering, 184(1): 99 – 123.

[47] S. Hüeber, B. Wohlmuth (2005). A primal-dual active set strategy for non-linear multibody contact problems. Computer Methods in Applied Mechanics and Engineering, 194: 3147–3166.

[48] S. Hüeber, B.I. Wohlmuth (2009). Thermo-mechanical contact problems on nonmatching meshes. Computer Methods in Applied Mechanics and Engineering, 198: 1338–1350.

[49] T.R.J. Hughes, R.L. Taylor, J. Sackman, A. Curnier, W. Kanoknukulchai (1976). A finite element method for a class of contact-impact problems. Computer Methods in Applied Mechanics and Engineering, 8(3): 249-276.

[50] T.J.R. Hughes, R.L. Taylor, W. Kanoknukulchai (1977). A finite element method for large displacement contact and impact problems. In: K. Bathe, J. Oden, W. Wunderlich (Eds.), Formulations and Computational Algorithms in Finite Element Analysis: U.S.– Germany Symposium, MIT, Cambridge, 468-495.

[51] T.J.R. Hughes, J.A. Cottrell, Y. Bazilevs (2005). Isogeometric analysis: CAD, finite elements, NURBS, exact geometry and mesh refinement. Computer Methods in Applied Mechanics and Engineering, 194: 4135–4195.

[52] J. Kiendl, K. Bletzinger, J. Linhard, R. Wüchner (2009). Isogeometric shell analysis with Kirchhoff–Love elements. Computer Methods in Applied Mechanics and Engineering, 198: 3902–3914.

[53] J. Kim and S. Youn (2012). Isogeometric contact analysis using mortar method. International Journal for Numerical Methods in Engineering, 89(12): 1559-1581.

[54] S.K. Kleiss, B. Jüttler, W. Zulehner (2012). Enhancing isogeometric analysis by a finite element-based local refinement strategy. Computer Methods in Applied Mechanics and Engineering, 213–216: 168–182.

[55] A. Konyukhov, K. Schweizerhof (2004). Covariant Description for Frictional Contact Problems. Springer.

[56] A. Konyukhov, K. Schweizerhof (2008). On the solvability of closest point projection procedures in contact analysis: analysis and solution strategy for surfaces of arbitrary geometry. Computer Methods in Applied Mechanics and Engineering, 197: 3045-3056.

[57] A. Konyukhov, K. Schweizerhof (2009). Incorporation of contact for high-order finite elements in covariant form. Computer Methods in Applied Mechanics and Engineering, 198: 1213–1223.

[58] A. Konyukhov, K. Schweizerhof (2012), Geometrically exact theory for contact interactions of 1D manifolds. Algorithmic implementation with various finite element models. Computer Methods in Applied Mechanics and Engineering, 205-208: 130–138.

[59] L. Krstulovic-Opara, P. Wriggers, J. Korelc (2002). A C1-continuous formulation for 3D finite deformation frictional contact. Computational Mechanics, 29: 27–42.

[60] R.L. Landon, M.W. Hast, S.J. Piazza (2009). Robust contact modeling using trimmed nurbs surfaces for dynamic simulations of articular contact. Computer Methods in Applied Mechanics and Engineering, 198: 2339-2346.

[61] T.A. Laursen (2002). Computational Contact and Impact Mechanics. Springer.

[62] T.A. Laursen, J. Simo (1993). A continuum-based finite element formulation for the implicit solution of multibody, large deformation-frictional contact problems. International Journal for Numerical Methods in Engineering, 36: 3451–3485.

[63] J. Lengiewicz, J. Korelc, S. Stupkiewicz (2010). Automation of finite element formulations for large deformation contact problems. International Journal for Numerical Methods in Engineering, 85: 1252-1279.

[64] W.N. Liu, G. Meschke, H.A. Mang (1999). A note on the algorithmic stabilization of 2d contact analyses. In: L. Gaul and C.A. Brebbia, editors, Computational Methods in Contact Mechanics IV, 231–240. Wessex Institute, Southhampton.

[65] J. Lu (2011). Isogeometric contact analysis: geometric basis and formulation for frictionless contact. Computer Methods in Applied Mechanics and Engineering, 200: 726–74.

[66] J. Lu and C. Zheng (2014). Dynamic cloth simulation by isogeometric analysis. Computer Methods in Applied Mechanics and Engineering, 268: 475–493.

[67] M.E. Matzen, T. Cichosz, M. Bischoff (2013). A point to segment contact formulation for isogeometric, NURBS based finite elements. Computer Methods in Applied Mechanics and Engineering, 255: 27–39.

[68] T. McDewitt, T. A. Laursen (2000). A mortar-finite element formulation for frictional contact problems. International Journal for Numerical Methods in Engineering, 48: 1525–1547.

[69] S. Morganti, F. Auricchio, D. Benson, F.I. Gambarin, S. Hartmann, T.J.R. Hughes, A. Reali (submitted). Patient-specific isogeometric structural analysis of aortic valve closure.

[70] V. Padmanabhan, T.A. Laursen (2001). A framework for development of surface smoothing procedures in large deformation frictional contact analysis. Finite Elements in Analysis and Design, 37: 173–198.

[71] P. Papadopoulos, R.L. Taylor (1992). A mixed formulation for the finite element solution of contact problems. Computer Methods in Applied Mechanics and Engineering, 94: 373–389.

[72] P. Papadopoulos, R.L. Taylor (1993). A simple algorithm for three-dimensional finite element analysis of contact problems. Computers & Structures, 46: 1107-1118.

[73] P. Papadopoulos, R.E. Jones, J.M. Solberg (1995). A novel finite element formulation for frictionless contact problems, International Journal for Numerical Methods in Engineering, 38: 2603-2617.

[74] L. Piegl, W. Tiller (1996). The NURBS Book. Springer, Berlin Heidelberg New York, 2nd edition.

[75] G. Pietrzak, A. Curnier (1999). Large deformation frictional contact mechanics: continuum formulation and augmented Lagrangean treatment. Computer Methods in Applied Mechanics and Engineering, 177: 351–381.

[76] A. Popp, M. Gee, W. Wall (2009). A finite deformation mortar contact formulation using a primal-dual active set strategy. International Journal for Numerical Methods in Engineering, 79: 1354–1391.

[77] M.A. Puso, T.A. Laursen (2002). A 3D contact smoothing method using Gregory patches. International Journal for Numerical Methods in Engineering, 54: 1161–1194.

[78] M.A. Puso, T.A. Laursen (2004). A mortar segment-to-segment frictional contact method for large deformations. Computer Methods in Applied Mechanics and Engineering, 193: 4891–4913.

[79] M.A. Puso, T.A. Laursen, J. Solberg (2008). A segment-to-segment mortar contact method for quadratic elements and large deformations. Computer Methods in Applied Mechanics and Engineering, 197: 555–566.

[80] M. Ruess, D. Schillinger, A.I. Özcan, E. Rank (2014). Weak coupling for isogeometric analysis of non-matching and trimmed multi-patch geometries. Computer Methods in Applied Mechanics and Engineering, 269: 46–71.

[81] D.F. Rogers (2001). An Introduction to NURBS with Historical Perspective. Morgan Kaufmann Publishers.

[82] R.A. Sauer (2013). Local finite element enrichment strategies for 2D contact computations and a corresponding post-processing scheme. Computational Mechanics, 52(2): 301-319.

[83] R.A. Sauer (submitted). Stabilized finite element formulations for liquid membranes and their application to droplet contact.

[84] R.A. Sauer, X.T. Duong, C.J. Corbett (2014). A computational formulation for constrained solid and liquid membranes considering isogeometric finite elements. Computer Methods in Applied Mechanics and Engineering, 271: 48-68.

[85] R.A. Sauer, L. De Lorenzis (2013). A computational contact formulation based on surface potentials. Computer Methods in Applied Mechanics and Engineering, 253: 369-395.

[86] R.A. Sauer, L. De Lorenzis (submitted). An unbiased computational contact formulation for 3D friction.

[87] D. Schillinger, J.A. Evans, A. Reali, M.A. Scott, T.J.R. Hughes (2013). Isogeometric collocation: cost comparison with Galerkin methods and extension to adaptive hierarchical NURBS discretizations. Computer Methods in Applied Mechanics and Engineering, 267: 170-232.

[88] D. Schillinger, L. Dedé, M.A. Scott, J.A. Evans, M.J. Borden, E. Rank, T.J.R. Hughes (2012). An isogeometric design-through-analysis methodology based on adaptive hierarchical refinement of NURBS, immersed boundary methods, and T-spline CAD surfaces. Computer Methods in Applied Mechanics and Engineering, 249-250 :116-150.

[89] M.A. Scott, M.J. Borden, C.V. Verhoosel, T.W. Sederberg, T.J.R. Hughes (2011). Isogeometric finite element data structures based on Bézier extraction of T-splines. International Journal for Numerical Methods in Engineering, 88(2): 126-156.

[90] M.A. Scott, X. Li, T.W. Sederberg, T.J.R. Hughes (2012). Local refinement of analysis-suitable T-splines. Computer Methods in Applied Mechanics and Engineering, 213–216: 206–222.

[91] M.A. Scott, D.C. Thomas, E.J. Evans (2014). Isogeometric spline forests, Computer Methods in Applied Mechanics and Engineering, 269: 222–264.

[92] T.W. Sederberg, J. Zheng, A. Bakenov, A. Nasri (2003). T-splines and T-NURCCs. ACM Transactions on Graphics - Proceedings of ACM SIGGRAPH 2003, 22(3): 477-484.

[93] J. Simo, P. Wriggers, R.L. Taylor (1985). A perturbed Lagrangian formulation for the finite element solution of contact problems. Computer Methods in Applied Mechanics and Engineering, 50: 163–180.

[94] M. Stadler, G.A. Holzapfel, J. Korelc (2003). C^n-continuous modelling of smooth contact surfaces using NURBS and application to 2D problems. International Journal for Numerical Methods in Engineering, 57: 2177–2203.

[95] B.A. Szabó, I. Babuška (1991). Finite element analysis. John Wiley & Sons, New York.

[96] B.A. Szabó, A. Düster, E. Rank (2004). The p-version of the Finite Element Method. In: E. Stein, R. de Borst, T.J.R. Hughes (eds.), Encyclopedia of Computational Mechanics, John Wiley & Sons, New York, 1(5): 119–139.

[97] R.L. Taylor, P. Papadopoulos (1991). On a patch test for contact problems in two dimensions. In: Computational Methods in Nonlinear Mechanics, P. Wriggers, W. Wanger (eds). Springer: Berlin, 690–702.

[98] R.L. Taylor, P. Wriggers (1999). Smooth surface discretization for large deformation frictionless contact. Technical report, University of California, Berkeley. Report No. UCB/SEMM-99-04.

[99] İ Temizer, P. Wriggers, T.J.R. Hughes (2011). Contact treatment in isogeometric analysis with NURBS. Computer Methods in Applied Mechanics and Engineering, 200(9–12): 1100–1112.

[100] İ. Temizer, P. Wriggers, T.J.R. Hughes (2012). Three-dimensional mortar-based frictional contact treatment in isogeometric analysis with NURBS. Computer Methods in Applied Mechanics and Engineering, 209-212: 115-128.

[101] İ Temizer (2014). Multiscale thermomechanical contact: Computational homogenization with isogeometric analysis. International Journal for Numerical Methods in Engineering, 97(8): 582-607.

[102] M. Tur, E. Giner, F. J. Fuenmayor, P. Wriggers (2012). 2D contact smooth formulation based on the mortar method. Computer Methods in Applied Mechanics and Engineering 247–248: 1–14.

[103] A.-V. Vuong, C. Giannelli, B. Jüttler, B. Simeon (2011). A hierarchical approach to adaptive local refinement in isogeometric analysis. Computer Methods in Applied Mechanics and Engineering, 200: 3554–3567.

[104] S.P. Wang, E. Nakamachi (1999). The inside-outside contact search algorithm for finite element analysis. International Journal for Numerical Methods in Engineering, 40: 3665–3685.

[105] B. Wohlmuth (2000). A mortar finite element method using dual spaces for the Lagrange multiplier. SIAM Journal on Numerical Analysis, 38: 989–1012.

[106] B. Wohlmuth (2001). Discretization methods and iterative solvers based on domain decomposition. Lecture Notes in Computational Science and Engineering, 17, Springer, Berlin.

[107] B. Wohlmuth, R. Krause (2003). Monotone multigrid methods on nonmatching grids for nonlinear multibody contact problems. SIAM Journal on Scientific Computing, 25: 324–347.

[108] P. Wriggers (2006). Computational Contact Mechanics. Springer.

[109] P. Wriggers, L. Krstulovic-Opara, J. Korelc (2001). Smooth C1-interpolations for two-dimensional frictional contact problems. International Journal for Numerical Methods in Engineering, 51: 1469–1495.

[110] P. Wriggers, J. Simo (1985). A note on tangent stiffness for fully nonlinear contact problems. Communications in Applied Numerical Methods, 1: 199–203.

[111] P. Wriggers, T. Van, E. Stein (1990). Finite element formulation of large deformation impact-contact problems with friction. Computers & Structures, 37: 319–333.

[112] P. Wriggers, G. Zavarise (2011). Preface to Lecture Notes in Applied and Computational Mechanics, 58.

[113] B. Yang, T.A. Laursen, X. Meng (2005). Two dimensional mortar contact methods for large deformation frictional sliding. International Journal for Numerical Methods in Engineering, 62: 1183–1225.

[114] G. Zavarise, L. De Lorenzis (2009a). The node-to-segment algorithm for 2D frictionless contact: classical formulation and special cases. Computer Methods in Applied Mechanics and Engineering, 198(41-44): 3428-3451.

[115] G. Zavarise, L. De Lorenzis (2009b). A modified node-to-segment algorithm passing the contact patch test. International Journal for Numerical Methods in Engineering, 79:379–416.

[116] G. Zavarise, P. Wriggers (1998). A segment-to-segment contact strategy. Mathematical and Computer Modelling, 28: 497–515.

	Partition of unity	Sign	Inter-element continuity	Interpolatory	Convex hull/ Var. dim.
Lagrange	yes	any	C^0	at the nodes	no
Bernstein	yes	≥ 0	C^0	at the inter-element boundary	yes
B-splines	yes	≥ 0	C^{p-1} (*)	at the patch boundary	yes
NURBS	yes	≥ 0	C^{p-1} (*)	at the patch boundary	yes

Tab. 1: Main properties of the basis functions illustrated in Section 2. (*) At unique knots.

	FEM	IGA
NTS	Hughes et al. (1976, 1977), Hallquist (1979), Benson and Hallquist (1990), etc. Reviewed in Zavarise and De Lorenzis (2009a)	Matzen et al. (2013)
GPTS	Fischer and Wriggers (2005, 2006)	Temizer et al. (2011) De Lorenzis et al. (2011) Dimitri et al. (2014)
GPTS 2hp	Papadopoulos et al. (1995) Sauer and De Lorenzis (2013, submitted)	Lu (2011)
Mortar	Belgacem et al. (1998), Hild (2000), Wohlmuth and Krause (2003), Puso and Laursen (2004), etc. Reviewed in Popp and Wall (this special issue)	Temizer et al. (2011, 2012) De Lorenzis et al. (2011, 2012) Kim and Youn (2012)

Tab. 2: Summary of contact formulations in the discretized setting.

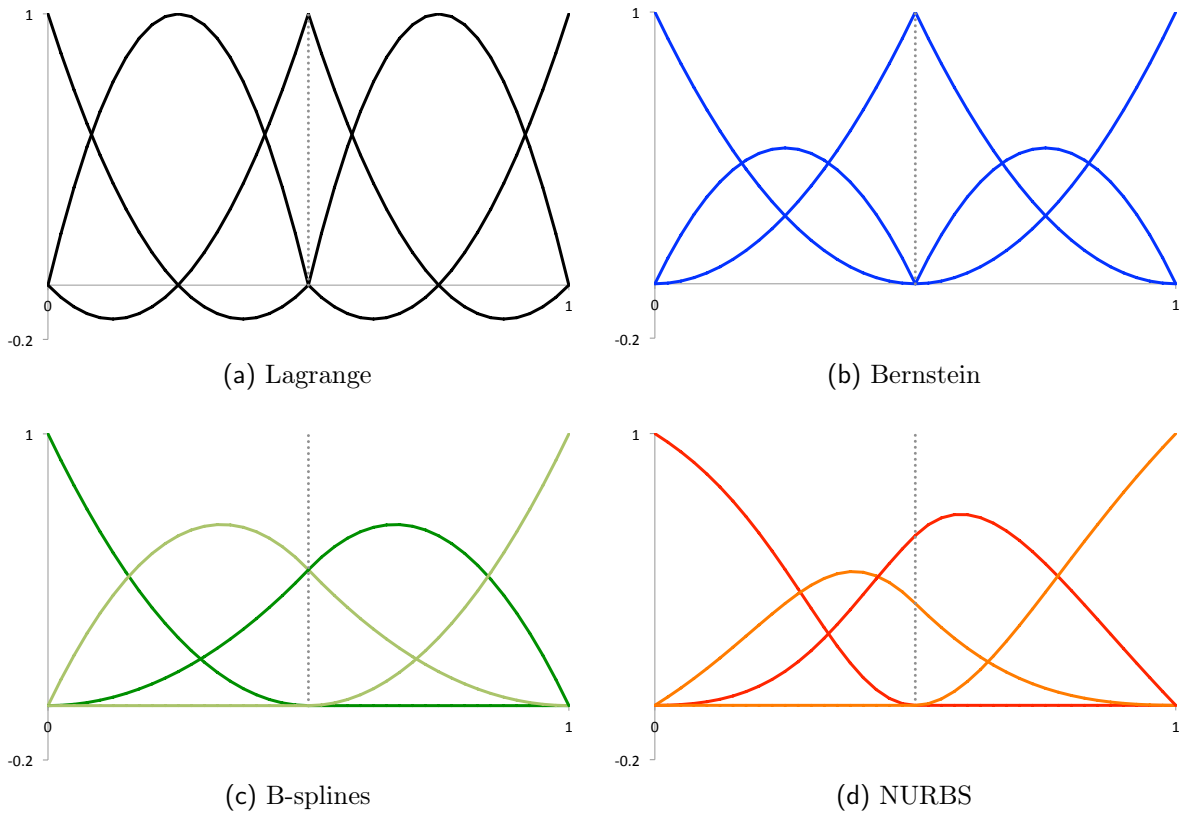

(a) Lagrange (b) Bernstein

(c) B-splines (d) NURBS

Fig. 1: Basis functions of degree $p = 2$ on a two-element parametric space ($\xi = 0.5$ corresponds to the element boundary). For B-splines and NURBS, the knot vector is $\Xi = \{0\,0\,0\,0.5\,1\,1\,1\}$. The NURBS basis functions have been assigned weights $w_1 = 1$, $w_2 = 0.3$, $w_3 = 0.5$, $w_4 = 1$.

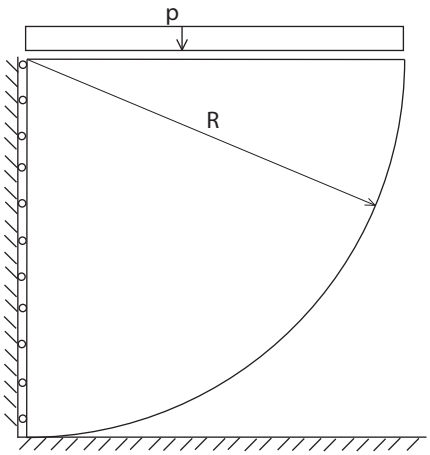

Fig. 2: Example 1.

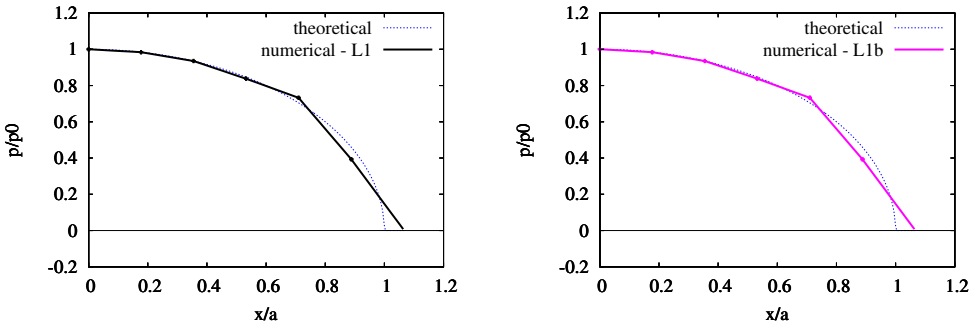

(a) L^1 (b) L^1_b

Fig. 3: Mesh with 24x24 elements, linear parameterizations.

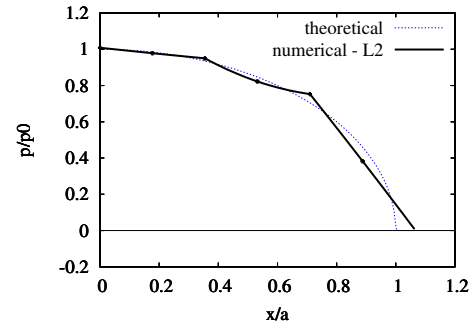

(a) L^2

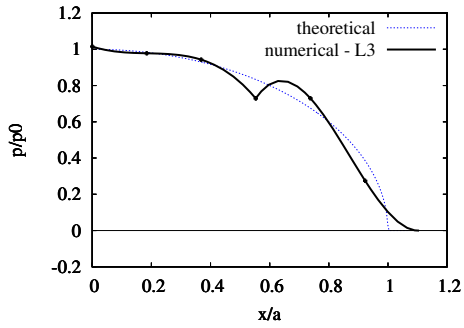

(b) L^3

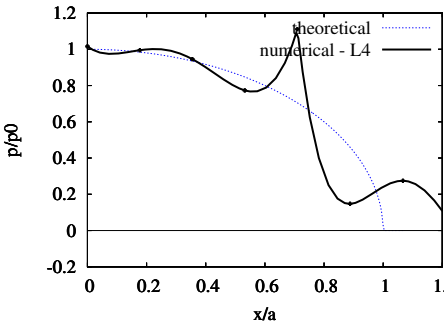

(c) L^4

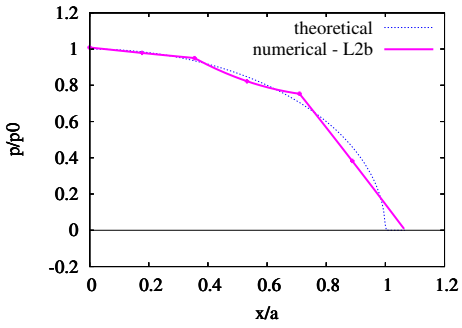

(d) L_b^2

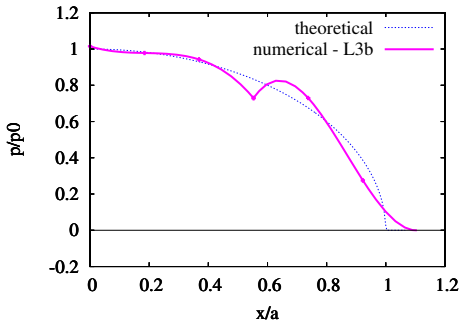

(e) L_b^3

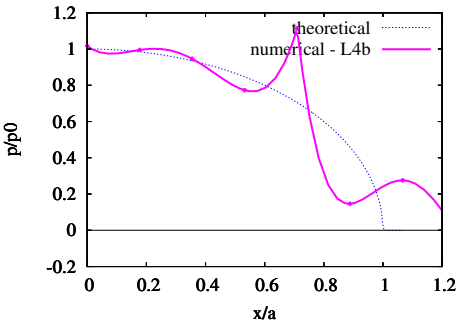

(f) L_b^4

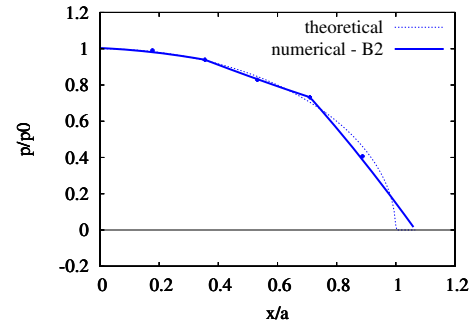

(g) B^2

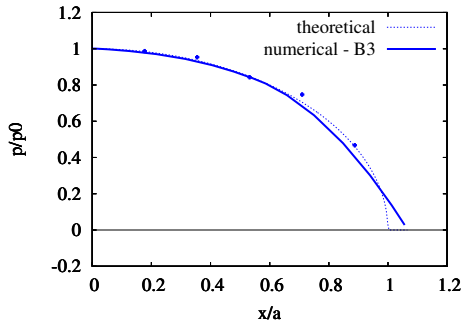

(h) B^3

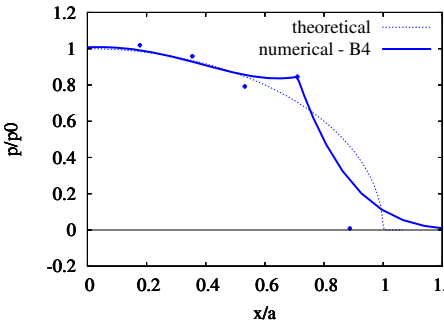

(i) B^4

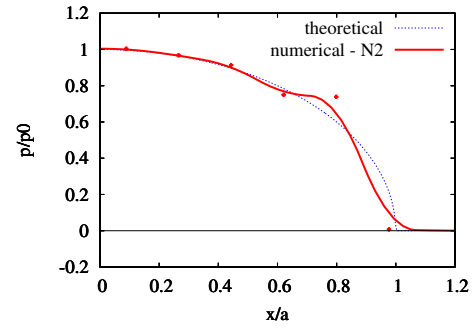

(j) N^2

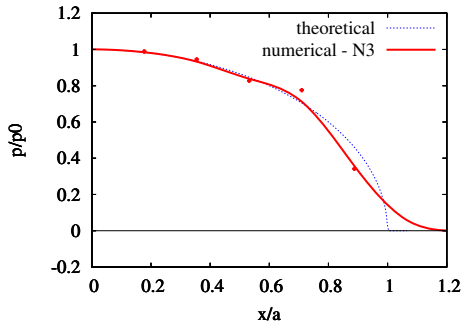

(k) N^3

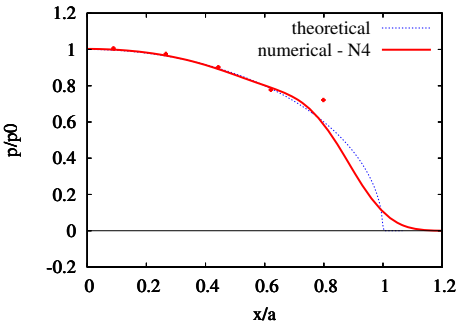

(l) N^4

Fig. 4: Mesh with 24x24 elements, higher order parameterizations.

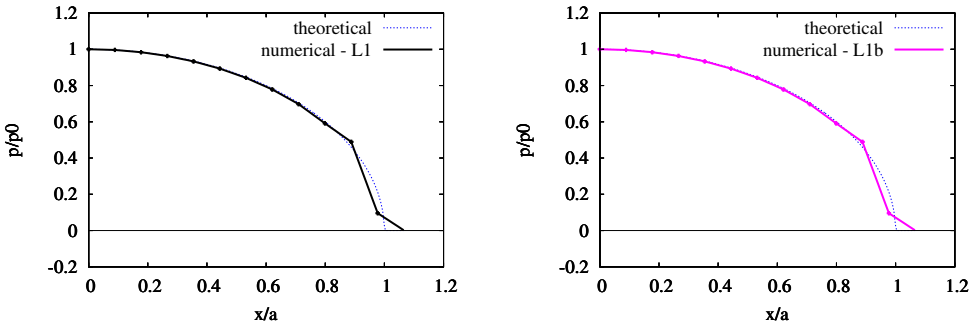

(a) L^1 (b) L^1_b

Fig. 5: Mesh with 48x24 elements, linear parameterizations.

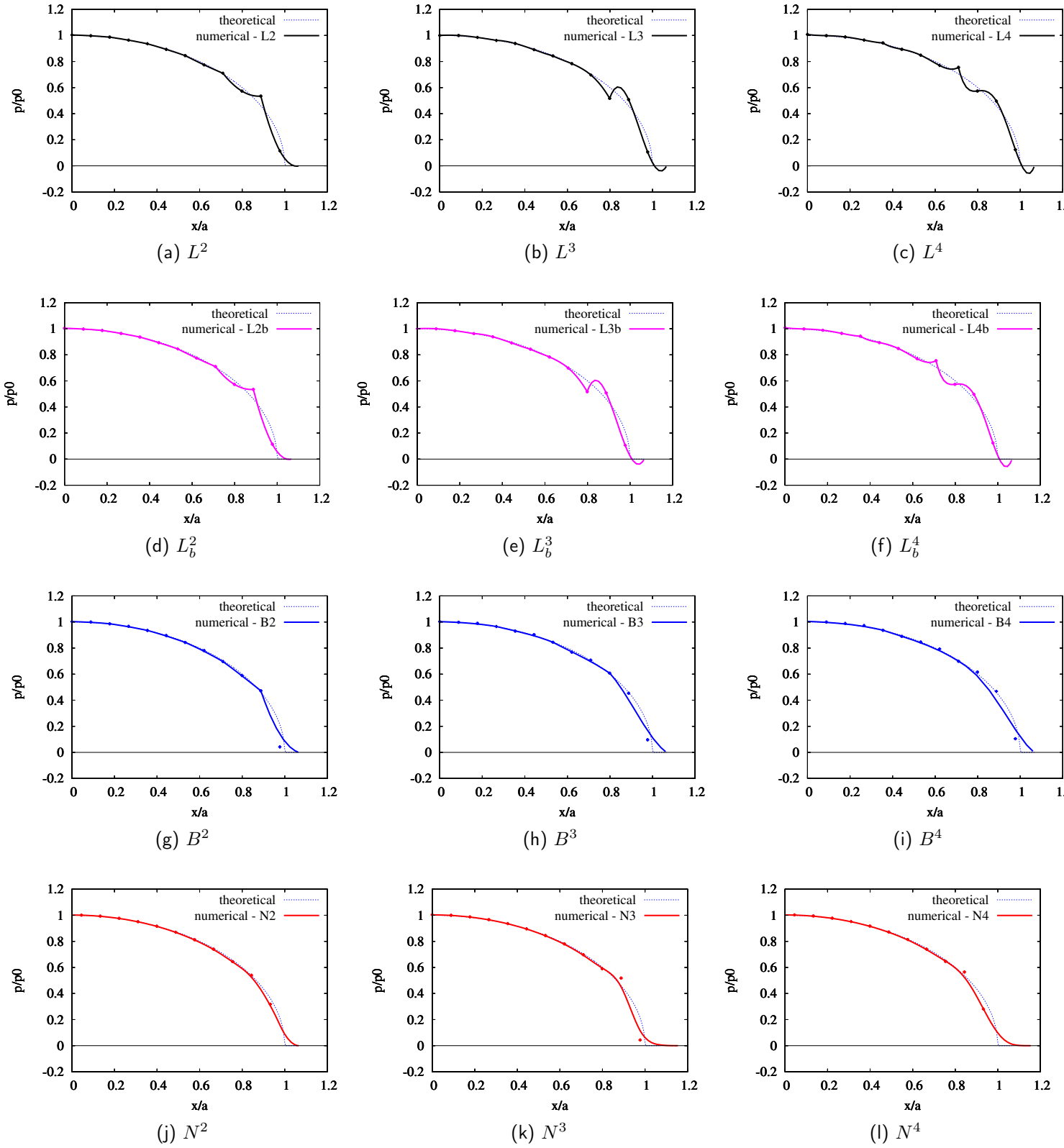

(a) L^2 (b) L^3 (c) L^4

(d) L_b^2 (e) L_b^3 (f) L_b^4

(g) B^2 (h) B^3 (i) B^4

(j) N^2 (k) N^3 (l) N^4

Fig. 6: Mesh with 48x24 elements, higher order parameterizations.

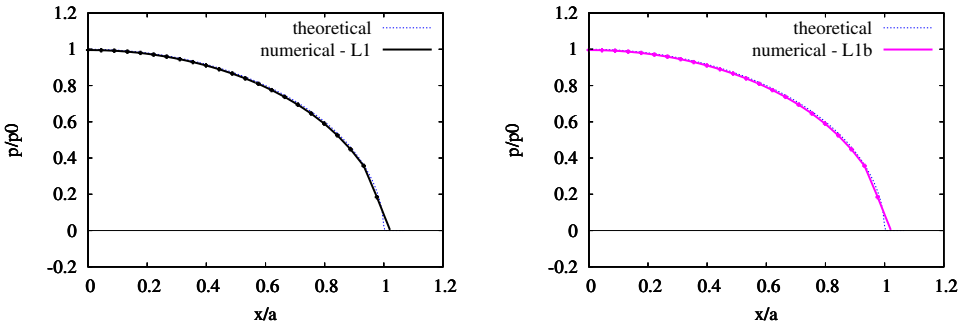

(a) L^1 (b) L^1_b

Fig. 7: Mesh with 96x48 elements, linear parameterizations.

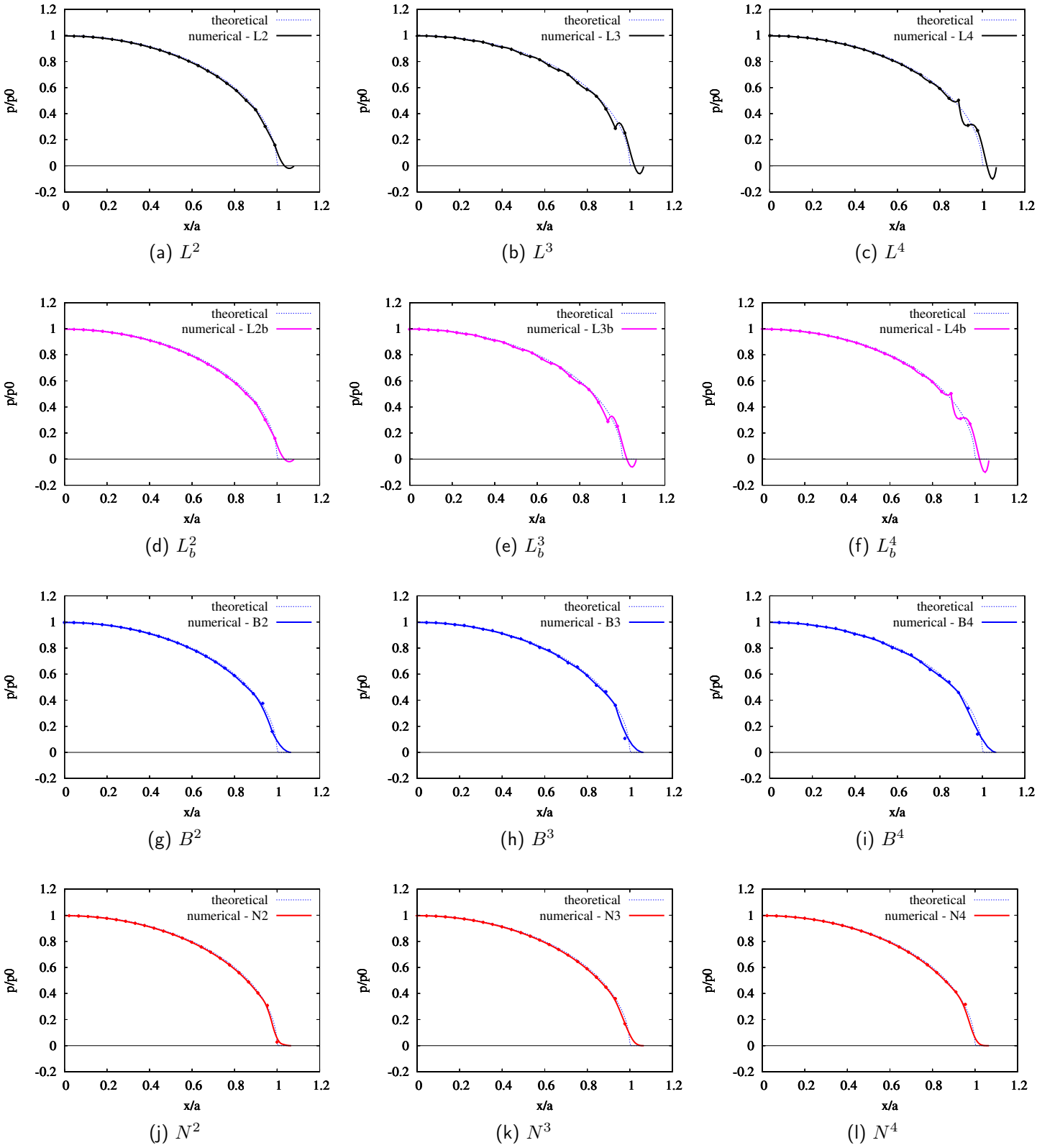

(a) L^2 (b) L^3 (c) L^4

(d) L_b^2 (e) L_b^3 (f) L_b^4

(g) B^2 (h) B^3 (i) B^4

(j) N^2 (k) N^3 (l) N^4

Fig. 8: Mesh with 96x48 elements, higher order parameterizations.

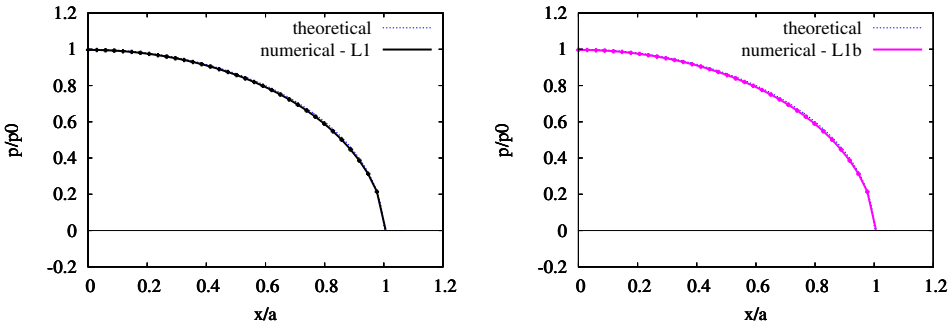

(a) L^1 (b) L^1_b

Fig. 9: Mesh with 144x48 elements, linear parameterizations.

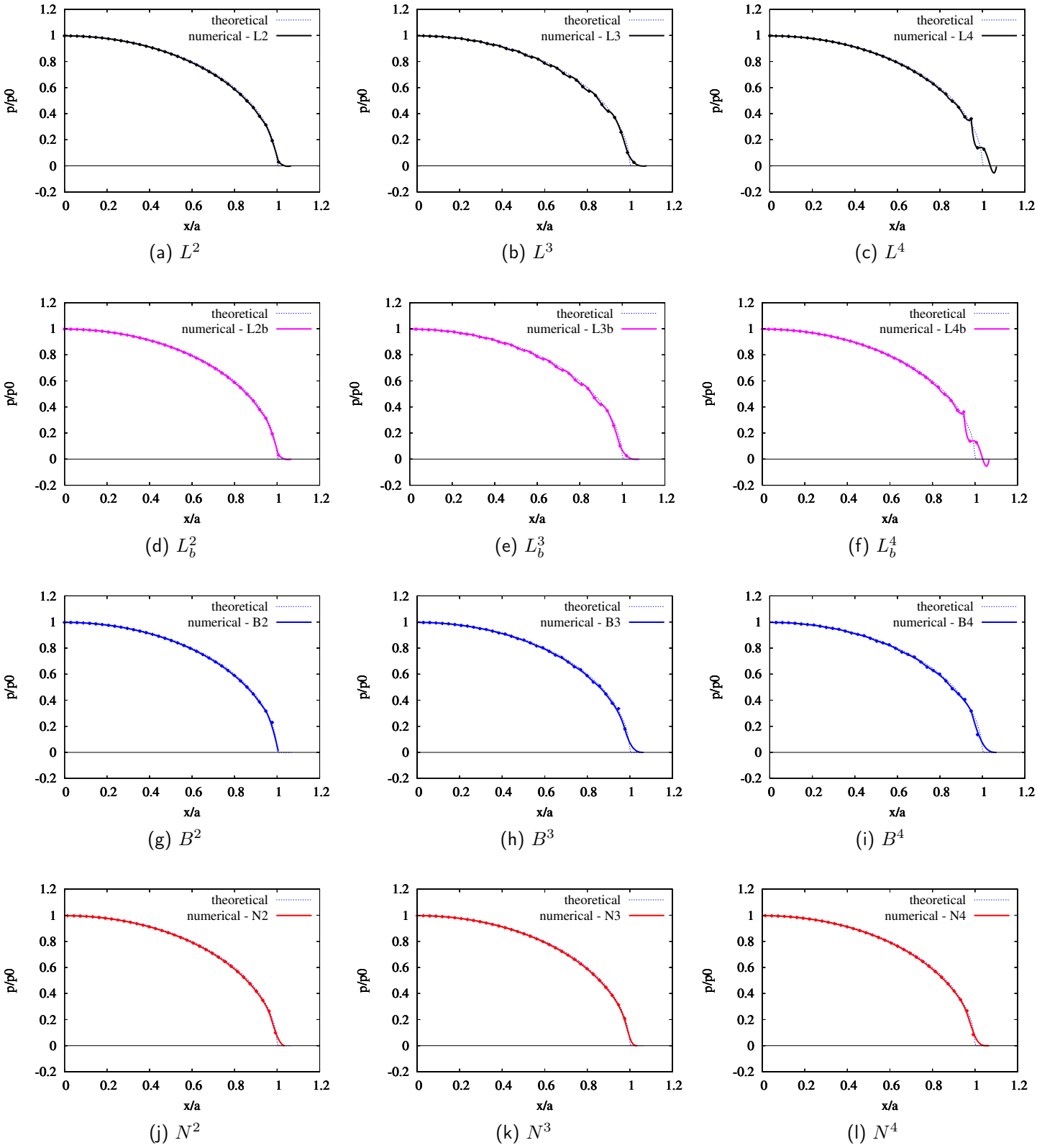

(a) L^2 (b) L^3 (c) L^4

(d) L_b^2 (e) L_b^3 (f) L_b^4

(g) B^2 (h) B^3 (i) B^4

(j) N^2 (k) N^3 (l) N^4

Fig. 10: Mesh with 144x48 elements, higher order parameterizations.

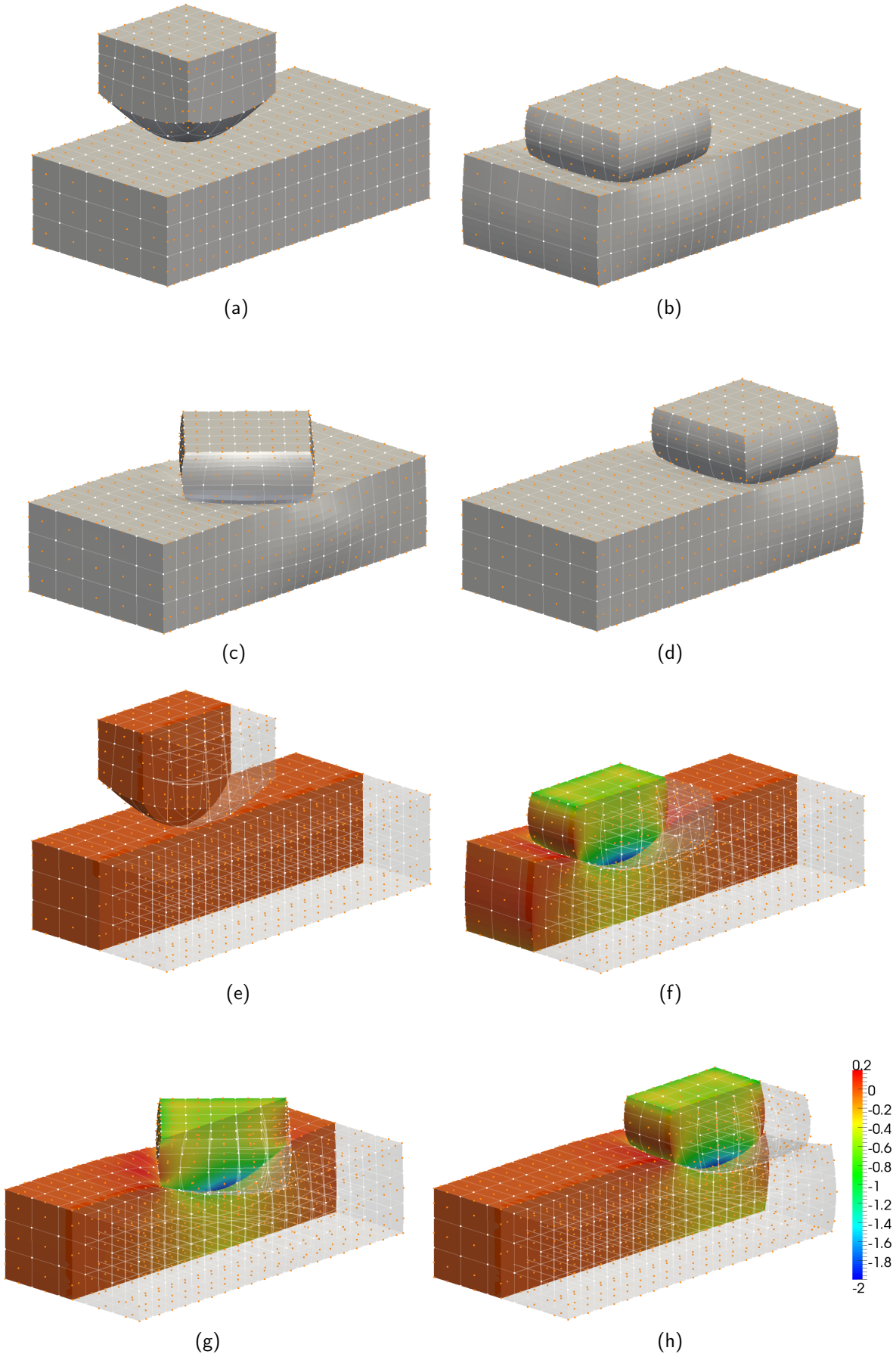

Fig. 11: Rotating ironing problem: snapshots of the analysis. The orange dots represent the control points and the white lines are the boundaries of the Bézier elements.

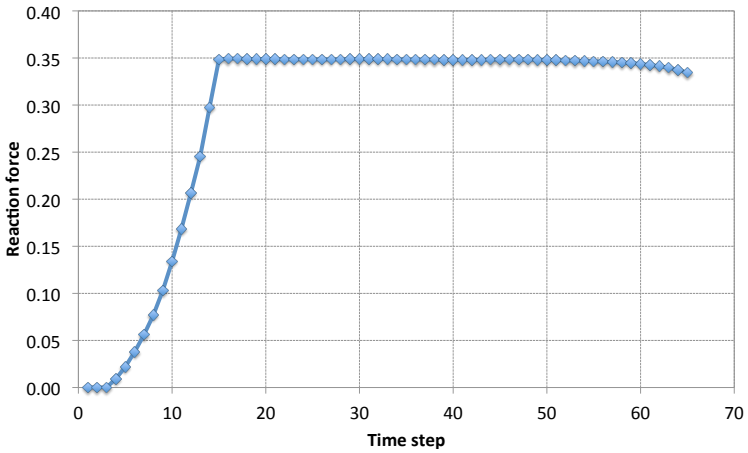

Fig. 12: Rotating ironing problem: vertical reaction history.